Published by Institute of Physics Publishing for SISSA

Received: *June 22, 2007*
Revised: *August 4, 2007*
Accepted: *September 19, 2007*
Published: *October 3, 2007*

Connecting LHC, ILC, and quintessence

Daniel J.H. Chung and Lisa L. Everett

Department of Physics, University of Wisconsin, Madison, WI 53706, U.S.A.
E-mail: danielchung@wisc.edu, leverett@wisc.edu

Kyoungchul Kong

Theoretical Physics Department, Fermilab, Batavia, IL 60510, U.S.A.
E-mail: kckong@fnal.gov

Konstantin T. Matchev

Institute for Fundamental Theory, University of Florida, Gainesville, FL 32611, U.S.A.
E-mail: matchev@phys.ufl.edu

Abstract: If the cold dark matter consists of weakly interacting massive particles (WIMPs), anticipated measurements of the WIMP properties at the Large Hadron Collider (LHC) and the International Linear Collider (ILC) will provide an unprecedented experimental probe of cosmology at temperatures of order 1 GeV. It is worth emphasizing that the expected outcome of these tests may or may not be consistent with the picture of standard cosmology. For example, in kination-dominated quintessence models of dark energy, the dark matter relic abundance can be significantly enhanced compared to that obtained from freeze out in a radiation-dominated universe. Collider measurements then will simultaneously probe both dark matter and dark energy. In this article, we investigate the precision to which the LHC and ILC can determine the dark matter and dark energy parameters under those circumstances. We use an illustrative set of four benchmark points in minimal supergravity in analogy with the four LCC benchmark points. The precision achievable together at the LHC and ILC is sufficient to discover kination-dominated quintessence, under the assumption that the WIMPs are the only dark matter component. The LHC and ILC can thus play important roles as alternative probes of both dark matter and dark energy.

Keywords: Beyond Standard Model, Supersymmetric Standard Model, Cosmology of Theories beyond the SM, Supersymmetry Phenomenology.

JHEP10(2007)016

Contents

1. Introduction

Current cosmological data [1 – 4] indicate that the energy density of the universe today is dominated by degrees of freedom beyond those of the Standard Model (SM) of particle physics, with approximately 73% given by dark energy, a form of energy characterized by negative pressure, and approximately 23% given by nonbaryonic dark matter. Given that future colliders such as the Large Hadron Collider (LHC) and International Linear Collider (ILC) are designed to probe physics beyond the SM, it is important to investigate whether and to what extent these experiments can probe these elusive forms of matter and energy.

For dark matter, it is well known that both direct and indirect collider physics connections can be established, depending on the properties of the dark matter candidate. One particularly well-motivated class of models is that in which the dark matter is a neutral weakly interacting massive particle (WIMP). Such particles are in thermal equilibrium in the early universe, and the standard freeze out calculation predicts a value for their relic density which is in the right ballpark as required by cosmology. WIMPs are naturally present in models which attempt to solve the gauge hierarchy problem, since such models generically introduce new weakly interacting particles. Prototype scenarios include models with softly broken $N = 1$ supersymmetry (SUSY), in which there is a conserved discrete symmetry, R-parity. In such models the lightest superpartner (LSP), typically a neutralino, is a viable cold dark matter candidate. The connections between astroparticle and collider physics have been extensively explored in the literature on supersymmetric dark matter [5 – 22]. More recently, other WIMP candidates have emerged in new physics

JHEP10(2007)016

scenarios which include a conserved discrete symmetry, such as models with flat [23, 24] or warped [25, 26] extra dimensions, and Little Higgs models [27 – 31].

It is much more difficult to establish a direct link to collider physics for the case of dynamical dark energy, since it is typically far more weakly coupled to the SM (for an example of an intriguing exception, see [32]). Although this energy density can be the cosmological constant, in which case cosmology has given us an invaluable clue to the cosmological constant problem, it is plausible that the dark energy can be associated with an effective scalar field degree of freedom, commonly called a quintessence field [33 – 37]. Collider experiments are unlikely to probe the unknown quintessence field directly, given its typical range of masses and couplings. Connections between collider physics and dark energy in the form of quintessence are thus necessarily indirect, and only a few are known. One connection is in the context of models with low energy supersymmetry. Since four-dimensional de Sitter space does not admit unbroken $N = 1$ supersymmetry [38], the discovery of supersymmetry through measurements of spins and couplings, and hints for its spontaneous breaking mechanism through measurements of mass patterns, will give us clues to the cosmological constant problem and possibly its associated quintessence dynamics. Other indirect connections with collider physics result because quintessence dynamics can leave an imprint on the cosmological history, which in turn determines an observable quantity that depends partly on parameters deduced from collider measurements.

One intriguing collider physics connection can arise through the gravitational interactions of the dark matter with quintessence. For thermal relics such as LSP dark matter, freeze out occurs when the expansion rate becomes larger than the interaction rate for reactions which change the LSP number density. In the standard cosmological scenario, freeze out represents the gravitational interactions between the cold dark matter and the relativistic gas of particles dominating the energy density of the universe at the time of freeze out. However, if the coherent field energy density of the quintessence field dominates during freeze out, freeze out now represents the gravitational interactions between the dark matter and the dark energy field degrees of freedom. In such cases, the relic density of the WIMP can be very strongly affected. More explicitly, the WIMP energy density today can be written as

$$\Omega_\chi h^2 \propto \left(\frac{T_{\rm today}}{m_\chi x_F}\right)^3 \left(\frac{m_\chi H_F}{\langle\sigma_A v\rangle}\right), \tag{1.1}$$

where H_F is the Hubble expansion rate at freeze out, m_χ is the mass of the WIMP, $\langle\sigma_A v\rangle$ is the thermally-averaged annihilation cross-section, $x_F \equiv T/m_\chi \sim 1/20$ for electroweak scale cross-sections (with only logarithmic dependences on H_F, $\langle\sigma_A v\rangle$, and m_χ), and $T_{\rm today}$ is the temperature of the cosmic microwave background (CMB) today. Eq. (1.1) demonstrates that if H_F is increased due to the quintessence energy density, the WIMP relic density can be enhanced for the same microphysics contained in $\langle\sigma_A v\rangle$. Note that eq. (1.1) also makes manifest the well-known property in standard cosmology that $\Omega_\chi h^2$ becomes approximately independent of the mass m_χ for a fixed $\langle\sigma_A v\rangle$, since in this case $H_F \sim x_F^2 m_\chi^2/M_{pl}$.

A challenge for such alternate scenarios is that standard big bang nucleosynthesis (BBN) constrains any extra contribution to the relativistic energy density. The quintessence energy density therefore has to be large during the time of WIMP freeze

JHEP10(2007)016

out ($T \sim O(1)\,\mathrm{GeV}$) and then dilute more quickly than radiation to become effectively irrelevant by the time that BBN commences ($T_0 \sim 10^{-3}\,\mathrm{GeV}$). As pointed out by Salati [39], this can occur for scenarios in which the universe is driven by the quintessence kinetic energy (the kination-dominated period) before BBN. (Related scenarios were also suggested before by [40, 41].) Long after BBN, the universe can enter a quintessence potential energy dominated regime. Such kination dominated freeze out scenarios are then consistent with standard cosmology and predict that the *standard* relic abundance computed from the parameters extracted from the next generation of colliders will be mismatched from the relic abundance deduced from observational cosmology. Indeed, the kination hypothesis is only one of many possibilities we must turn to if future experiments find a mismatch between the standard computations of the relic abundance and cosmological observations.

The implications of kination domination for LSP dark matter have been explored previously [42 – 48]. We extend this work by analyzing the precision to which the LHC and ILC can *simultaneously* probe dark matter and dark energy. While colliders have traditionally been viewed as tools for discriminating among different *particle physics* models, we shall demonstrate that they are also capable of achieving sufficient precision on the effective field theory parameters to discern the difference between different *cosmological* models, e.g. the standard scenario and the kination domination scenario. The anticipated collider data will allow us to probe in the laboratory a new era in cosmological history, which may lead to significant deviations from the standard cosmological picture [49 – 52].

The order of presentation will be as follows. We begin by providing an overview of the issue of experimental tests of the WIMP hypothesis in section 2. In section 3, we review the effect of kination-dominated quintessence on the calculation of the WIMP thermal relic abundance, and provide a simple map between the kination scenario and the standard cosmological scenario. In section 4 we then investigate the capabilities of the LHC and ILC in pinning down both the dark matter and quintessence parameters. Following recent ILC studies, we use study points defined within the "mSUGRA" or "cMSSM" supersymmetric framework, where the superpartner masses are assumed to unify at the grand unification scale. Our study points are analogous to the set of four LCC study points (see e.g. [18]) which were chosen to represent the four "good" dark matter regions of the mSUGRA model. We reserve section 5 for our discussion and conclusions.

2. Colliders as dark matter and dark energy probes

We begin by discussing in general terms how high energy colliders can test the WIMP hypothesis. The physics process which determines the present dark matter relic anbundance, is the dark matter annihilation into *all* possible final states with SM particles. Once we know the total annihilation cross-section σ_A of any given WIMP candidate, we can straightforwardly predict its relic abundance. Therefore, we can test the WIMP hypothesis by studying the properties of the WIMP candidates, and consequently, trying to constrain their annihilation cross-section σ_A.

This is clearly a challenging exercise since colliders are not recreating the process of dark matter annihilation per se. Instead, given sufficient energy, colliders would produce

JHEP10(2007)016

WIMP dark matter particles, either directly or indirectly (in the decays of other particles). If those signals can be identified over the SM backgrounds, they can be studied in order to determine the properties of the dark matter particle, most notably, its mass and interaction strength to the different SM particles. It is in this sense that colliders are helpful in probing the dark matter.

However, it is clear that the extrapolation from collider data to a prediction about the dark matter annihilation cross-section σ_A is rather challenging. The main problem is that the relic abundance is determined by a multitude of final states, while at colliders we typically observe the dark matter particles only in a limited number of exclusive final states. It is unrealistic to expect that colliders will be able to measure every single dark matter coupling, and the best one could hope for is that the colliders will be able to measure the largest (and therefore most relevant) couplings with some precision, while placing limits on the remaining (hopefully smaller and less relevant) couplings. Obviously, the way this is done is by either observing a dark matter signal in a specific channel, which would provide a measurement of the corresponding coupling, or failing to observe a signal in a specific channel which would provide an upper limit on the corresponding coupling. Then, by adding the results for all possible annihilation final states, one would obtain both a lower limit $\sigma_A^{\min}$ and an upper limit $\sigma_A^{\max}$ on the *total* annihilation cross-section σ_A. Assuming standard cosmology, these limits would correspondingly translate into an upper and lower limit on the WIMP relic density Ω_χ. From the preceding discussion it is clear that $\sigma_A^{\min}$ (and the corresponding upper limit on Ω_χ) is derived from collider information from channels which *have been observed* while $\sigma_A^{\max}$ (and the lower limit on Ω_χ) is derived from collider information from channels which have *not* been observed. It is therefore also clear that the collider information about $\sigma_A^{\min}$ is more robust than the information regarding $\sigma_A^{\max}$. First, the presence of additional annihilation channels into non-SM final states would invalidate a bound on $\sigma_A^{\max}$ which had been derived strictly within the SM. Second, arriving at a meaningful bound on $\sigma_A^{\max}$ is *experimentally* quite challenging: the unobserved channels typically outnumber the observed ones, and also, the unobserved channels tend to be plagued with larger backgrounds and, correspondingly, larger uncertainties — after all, the large backgrounds are often the reason those channels have not been observed in the first place.

With all this in mind, let us now turn our attention to some specific scenarios. For any given WIMP dark matter candidate cosmology data provides a preferred value $\sigma_A^{\exp}$ for its *total* annihilation cross-section. This value depends mostly on whether the dark matter particle is an s-wave or p-wave annihilator, and is almost insensitive to the dark matter particle spin [53]. The test of dark matter at colliders is being done by comparing $\sigma_A^{\exp}$ to the derived limits on $\sigma_A^{\min}$ and $\sigma_A^{\max}$ as described above. Generally speaking, there are three possible outcomes of this test, which we shall now consider in turn.

(i) The test will be deemed successful if it turns out that

$$\sigma_A^{\min} < \sigma_A^{\exp} < \sigma_A^{\max}. \tag{2.1}$$

Under those circumstances, the dark matter particle discovered at colliders can solely account for all of the dark matter in the universe, i.e., there is no need for another

independent dark matter candidate. This is the scenario which has attracted the most attention in the literature. The gap between $\sigma_A^{\rm min}$ and $\sigma_A^{\rm max}$ is indicative of the precision with which colliders can test the WIMP dark matter hypothesis, and with the availability of a next generation lepton collider, typically the amount of wiggle room between $\sigma_A^{\rm min}$ and $\sigma_A^{\rm max}$ is reduced to the order of the current uncertainty in $\sigma_A^{\rm exp}$. If this turns out to be the case, we will have a triumphant confirmation of the WIMP dark matter hypothesis, although one could always find some caveats.[1]

Our major point here is that even though this case has been most widely considered in the literature, one should still pay proper attention to the other two possible outcomes below, especially since they would clearly indicate the presence of some additional new physics.

(ii) It is also quite possible that the collider test of dark matter will reveal that

$$\sigma_A^{\rm min} < \sigma_A^{\rm max} < \sigma_A^{\rm exp}. \tag{2.2}$$

Under the conventional interpretation, the dark matter candidate would then overclose the universe and cannot constitute the present-day cosmological dark matter. This conclusion is also subject to caveats either on the astrophysics or particle physics side. First, nonstandard cosmological evolution will change the picture - for example late inflation may dilute the dark matter density so that the particle observed at colliders is indeed the dark matter. This scenario can be strengthened by the observation of a direct detection signal of dark matter with mass in the range observed at colliders. The information obtained at colliders will then provide invaluable insights into early universe cosmology. Alternatively, one may look for particle physics resolutions of the puzzle. One possible explanation is that the WIMP dark matter candidate found at colliders is metastable and decays post-freeze out to a lighter particle with only gravitational interactions (superWIMP), which is the real dark matter [54, 55]. The mass ratio of the WIMP and the superWIMP can be adjusted to compensate for the overclosure of the universe and obtain the proper relic density today, although significant constraints arise from BBN and large scale structures. Colliders are very useful in providing information, such as the mass of the dark matter superWIMP, which cannot be obtained by any other means. Indeed, direct and indirect detection experiments are bound to fail in their searches for purely gravitationally interacting particle dark matter. Another possible particle physics explanation is to invalidate the bound $\sigma_A^{\rm max} < \sigma_A^{\rm exp}$. For example, additional invisible annihilation channels not easily revealed at colliders would push the bound on $\sigma_A^{\rm max}$ higher. In summary, outcome (2.2) requires either a reconcilation of the collider results by modifying standard cosmology and/or postulating new physics, or an invalidation of the colllider results by postulating new physics. New physics is thus expected either on the cosmology or particle physics side.

[1] For example, it would be very interesting to see how one could reconcile such a successful test of dark matter at colliders with a possible experimental direct detection of dark matter in a mass range different from the mass range found at colliders.

JHEP10(2007)016

(iii) The third possible outcome of the dark matter test at colliders is that

$$\sigma_A^{\rm exp} < \sigma_A^{\rm min} < \sigma_A^{\rm max}. \tag{2.3}$$

The conventional interpretation of this outcome is that the dark matter particle observed at colliders is not the only component of the dark matter in the universe, and one must look for another, yet unobserved, dark matter particle. Here again one may look for ways to circumvent this conclusion. On the astrophysics side, a non-standard cosmological history which leads to an enhancement of the relic abundance of the dark matter candidate, as is provided by the kination-dominated scenarios considered in this paper, can naturally accommodate this apparently unsuccessful dark matter particle candidate. On the particle physics side, one would have to invent another, independent dark matter candidate, which would provide the missing component of the dark matter. While this is possible in principle, it requires nonminimal model building - the presence of multiple dark matter candidates would require the existence of multiple conserved symmetries to ensure separately the stability of these particles on cosmological scales. Just as before, one may think of ways to invalidate the problematic bound $\sigma_A^{\rm exp} < \sigma_A^{\rm min}$. However, and this is the major difference between outcomes (2.2) and (2.3) from a particle physicist's perspective, it is clearly almost impossible to invalidate the lower bound on the annihilation cross-section, since, as elaborated above, it is derived from processes which have already been firmly observed at colliders, so any channels which may have been missed, would only increase $\sigma_A^{\rm min}$ and thus make the discrepancy worse. The outcome (2.3) is also very exciting for an astrophysicist, since, in the absence of alternative particle dark matter candidates, it would provide a direct indication of a cosmological relic abundance enhancement mechanism (such as kination domination) and give reasons to hunt for further correlated astrophysical/cosmological signatures [56, 44].

The above discussion underscores the potential importance of high energy colliders for the understanding of our universe. Colliders have traditionally been viewed as tools for *proving* that the WIMP particle indeed constitutes the dark matter. Now we also see that a potential unexpected outcome of the collider tests of the WIMP dark matter hypothesis may provide precious insights into early universe cosmology.

At the same time, one should not undervalue the potential significance of experiments dedicated to direct dark matter searches. A positive signal in any one of them would have several important implications. First and foremost, it would mean that the dark matter is real and would eliminate simple alternative explanations such as MOND or modified gravity. Of course, modified gravity can still play a role in the dark matter story in the second and third possible outcomes of the dark matter test at colliders stated above (see e.g. [45, 57]), but particle dark matter must play a significant role in gravitational clustering and galaxy formation. Second, it would boost the WIMP dark matter hypothesis, as it can (depending on the inferred relic density) rule out particles with purely gravitational interactions as a significant component of the dark matter halo (e.g. [58, 59, 54, 55]). Finally, as emphasized in [10, 18, 19], direct detection experiments will provide an important

piece of the dark matter puzzle – an independent estimate of the mass of the dark matter particle, which can then be contrasted with the analogous measurement at colliders. In the spirit of our earlier discussion, here again we can consider three possible outcomes of this comparison:

(i) It may turn out that the WIMP candidate found at colliders is *lighter* than the directly detected dark matter particle. This scenario would lead to several interesting possible interpretations. For example, the assumption that the dark matter is made up of a single component would imply that the particle found at colliders cannot be a dark matter particle and would have to decay outside the detector. Alternatively, the dark matter may be made up of several components, allowing for the coexistence of several particles as stable dark matter candidates. The collider particle may even be the dominant component if its direct detection rates are suppressed. In any case, the direct detection results would then provide a rough target for the next energy scale which would need to be reached and probed by collider experiments.

(ii) Conversely, it may turn out that the WIMP candidate found at colliders is *heavier* than the directly detected dark matter particle. Within the single component dark matter scenario, the most natural explanation of the discrepancy would be that the collider WIMP decays invisibly to the dark matter particle. Then, it would be interesting to go back and scour the collider data for events where the lighter dark matter particle can directly manifest itself.

(iii) Finally, the collider and astroparticle mass determinations may turn out to be in agreement, which would point towards a single WIMP dark matter component. The collider measurements of the dark matter particle properties can then be used to reconstruct the WIMP annhilation rate in the early universe. The outcome of this exercise is extremely interesting. For example, either $\sigma_A^{\rm max} < \sigma_A^{\rm exp}$ or $\sigma_A^{\rm exp} < \sigma_A^{\rm min}$ would necessarily require nonstandard cosmology. If $\sigma_A^{\rm max} < \sigma_A^{\rm exp}$, the universe appears overclosed and some mechanism of late entropy production (such as a phase transition or a late particle decay) is required. If, on the other hand, $\sigma_A^{\rm exp} < \sigma_A^{\rm min}$, the dark matter abundance would require some kind of a boost, such as a period of kination domination as will be discussed in this paper.

To summarize, the outcome of experimental tests of the WIMP hypothesis will provide significant insights into new physics. Although most studies of this issue focus on scenarios in which standard cosmology holds and the thermal WIMP discovered at colliders is the dominant component of the cold dark matter, such that $\sigma_A^{\rm min} < \sigma_A^{\rm exp} < \sigma_A^{\rm max}$, alternative outcomes also warrant careful consideration. Such alternative outcomes can have important implications for new particle physics, such as the possibility of several distinct constituents of the cold dark matter, and/or cosmology, such as the possiblity of cosmological enhancement or dilution mechanisms for the Hubble expansion of the universe. We focus here on a particular cosmological enhancement mechanism for the dark matter relic abundance due to the presence of dark energy in the form of quintessence. In this situation, $\sigma_A^{\rm exp} < \sigma_A^{\rm min} < \sigma_A^{\rm max}$, and yet the thermal WIMP measured at colliders can be the dominant

JHEP10(2007)016

component of the cold dark matter. Kination-dominated quintessence generically can be tested through a number of correlated cosmological implications and signatures (see [56] for a discussion and further details), but is also a framework in which dark energy can make itself manifest at high energy colliders, in striking contrast to the vast majority of known dark energy models. We will now concentrate on this scenario and explore the prospects for experimental tests at the LHC and ILC.

3. Cosmology and the dark matter/dark energy connection

Given the motivation for considering quintessence models of dark energy which include a period of kination domination, we turn to its effects on the dark matter relic abundance, as first discussed in [39]. In this section, we provide a self-contained set of analytic equations which can be used to map any ordinary dark matter freeze out scenario to the dark matter freeze out scenario of kination domination.[2]

In the usual thermal WIMP dark matter scenario (see e.g. [60]), the dark matter χ is assumed to be initially in chemical equilibrium with the thermal plasma that is in equilibrium with the photons. The WIMPs remain in equilibrium as long as the annihilation reaction rate $\Gamma_A \equiv n_\chi \langle \sigma_A v \rangle$ (σ_A is the cross section for reactions that change the number density n_χ and the averaging is with respect to a thermal ensemble) is much larger than the expansion rate of the universe $H \equiv \dot{a}/a$ (a is the scale factor). However, when Γ_A falls below H, n_χ no longer tracks the equilibrium density and $n_\chi a^3$ is nearly an adiabatic constant. This transition from equilibrium abundance tracking to a nearly adiabatic constant behavior is known as the freeze out transition. Typically, the energy density that governs H during the freeze out period is composed of relativistic degrees of freedom in equilibrium with the photons.

The assumption that the dark energy is in the form of quintessence naturally leads one to question whether the relativistic degrees of freedom governing the expansion rate H need be in chemical equilibrium with the photons during WIMP freeze out. Indeed, since the coupling of the quintessence field to ordinary matter needs to be very weak to maintain a long dynamical time scale and evade fifth force constraints, quintessence naturally never reaches chemical equilibrium with the photons. However, if the quintessence field were to dominate the universe during freeze out, its energy density must dilute faster than the energy density of the SM relativistic degrees of freedom ρ_R to evade the BBN constraint on the number of relativistic degrees of freedom. This constraint can be expressed (at 95% confidence level) as [61]

$$\Delta g_{*S} \lesssim 1.5 \frac{7}{4}, \tag{3.1}$$

where Δg_{*S} is the number of effective degrees of freedom [60] other than the photons, electrons, and neutrinos entering the total entropy density

$$s = \frac{2\pi^2}{45}(10.75 + \Delta g_{*S}) T_0^3, \tag{3.2}$$

[2]Here we will restrict our attention to a flat FRW universe with $ds^2 = dt^2 - a^2(t) d\vec{x}^2$ governed by the standard Einstein-Hilbert gravitational action. Planck's constant is defined to be $M_{pl} \approx 1.22 \times 10^{19}$GeV.

where T_0 is the temperature during BBN.

As pointed out in [39] , one way to achieve this is to have a period of kination domination, in which the kinetic energy of the quintessence field Φ dominates the energy density: $\rho_\Phi \approx \frac{1}{2}\dot{\Phi}^2 \gg \rho_R$. In this case, the energy density scales as

$$\frac{\rho_\Phi}{\rho_R} \propto \frac{1}{a^2}. \tag{3.3}$$

This indicates that if the ratio of energy density of Φ and photons at the temperature of 1 MeV is

$$\eta_\Phi \equiv \frac{\rho_\Phi}{\rho_\gamma}|_{T=1\mathrm{MeV}}, \tag{3.4}$$

the ratio at the time of freeze out is of the order

$$\frac{\rho_\Phi}{\rho_\gamma}|_{T=1\mathrm{GeV}} \sim 10^6 \eta_\Phi. \tag{3.5}$$

This indicates that the Φ energy density dominates over that of the relativistic degrees of freedom, since $\rho_\Phi \sim 10^5 \eta_\Phi \rho_R$ at the approximate period of freeze out and

$$0 \leq \eta_\Phi \lesssim 1. \tag{3.6}$$

Therefore, we can easily arrange ρ_Φ to control the freeze out temperature T_K in the kination dominated scenario. (Note that one should distinguish between ρ_γ which is the density of photons and ρ_R which is the energy density of all relativistic particles.)

Following the computational approach of [39], we can easily give a map between the dark matter abundance of the standard scenario and that of the kination domination scenario. With LSP dark matter in mind, the thermal averaged annihilation cross section (defined to be proportional to the number changing reaction rate) is

$$\langle \sigma_A v \rangle = \tilde{a} + \tilde{b}x, \tag{3.7}$$

where

$$x \equiv \frac{T}{m_\chi}, \tag{3.8}$$

m_χ is the mass of the WIMP, and $\tilde{a}$ ($\tilde{b}$) is the s-wave (p-wave) contribution to the annihilation cross section. The freeze out temperature parameter will be denoted by x_U in the standard scenario and x_K in the kination domination scenario. These quantities are defined by the equations

$$(\tilde{a} + \tilde{b}x_{U,K}) n_\chi^{eq}(x_{U,K}) = \frac{2}{x_{U,K}} H_{U,K}(x_{U,K}), \tag{3.9}$$

$$n_\chi^{eq}(x) = 2m_\chi^3 \left(\frac{x}{2\pi}\right)^{3/2} e^{-\frac{1}{x}}, \tag{3.10}$$

$$H_U(x) = \sqrt{\frac{8\pi^3}{90} g_*(x)} \frac{m_\chi^2}{M_{pl}} x^2, \tag{3.11}$$

$$H_K(x) = \sqrt{\frac{8\pi^3}{90} g_*(x)} \frac{m_\chi^2}{M_{pl}} x^2 \sqrt{1 + \alpha x^2}, \tag{3.12}$$

JHEP10(2007)016

where $g_*(x)$ is defined by the equation for the radiation energy density

$$\rho_R = \frac{\pi^2}{30} g_*(x) x^4 m_\chi^4. \tag{3.13}$$

In the kination domination scenario, the relic abundance today Ω_K can then be expressed relative to the usual relic abundance Ω_U as

$$\frac{\Omega_K}{\Omega_U} = \frac{\mu_U}{\mu_K} \frac{x_U^2}{x_K^2} \sqrt{\frac{g_*(x_U)}{g_*(x_K)}} \sqrt{1+\alpha x_K^2} \left[\frac{\tilde{a} + \tilde{b} x_U}{\tilde{a} + \tilde{b} x_K} \right], \tag{3.14}$$

$$\mu_U = 1 + \frac{2}{x_U} \left(\frac{\tilde{a} + \tilde{b} x_U/2}{\tilde{a} + \tilde{b} x_U} \right), \tag{3.15}$$

$$\mu_K = 1 + \frac{2}{x_K} \sqrt{1+\alpha x_K^2} \left(\frac{\tilde{a} A(u) + \tilde{b} x_K B(u)}{\tilde{a} + \tilde{b} x_K} \right), \tag{3.16}$$

$$A(u) = \frac{1}{u} \ln[u + \sqrt{1+u^2}], \tag{3.17}$$

$$B(u) = \frac{\sqrt{1+u^2} - 1}{u^2}, \tag{3.18}$$

$$u = \sqrt{\alpha} x_K \tag{3.19}$$

$$\alpha = \eta_\Phi \frac{m_\chi^2}{[g_*(T_0)/2] T_0^2} \left[\frac{g_*(T_K)}{g_*(T_0)} \right]. \tag{3.20}$$

In the above formulas, a subscript U denotes quantities associated with the usual freeze out scenario, while a subscript K denotes quantities associated with the kination domination scenario. Here the number of relativistic degrees of freedom governing the energy density g_* obeys the approximate relationship $g_* \approx g_{*S}$ (e.g. $g_*(T_K) \approx 90$ and $g_*(T_0) \approx 10.75$), and $T_0 = 1$ MeV is the temperature relevant for BBN (as opposed to the temperature today).

Assuming that $\eta_\Phi \leq 1$ is sufficiently large such that kination dominates at freeze out, let us approximate eq. (3.14) in the limit of either s-wave ($\tilde{a} \gg \tilde{b} x_K$) or p-wave ($\tilde{a} \ll \tilde{b} x_K$) dominance to obtain intuition for the type of enhancement obtained for kination domination. This is useful because in any given realistic model the dark matter candidate tends to be either a predominantly p-wave annihilator (e.g. the neutralino in supersymmetry) or an s-wave annihilator (e.g. the dark matter candidate in most other cases). For a p-wave annihilator we obtain

$$\frac{\Omega_K}{\Omega_U} \sim \frac{g_{*S}(T_U)}{g_{*S}(T_0)} \frac{T_U^2}{T_K T_0} \frac{\sqrt{\eta_\Phi}}{\sqrt{2 g_*(T_U)}}. \tag{3.21}$$

The powers of the temperature T in eq. (3.21) can be understood as follows. Since $\Omega_{U,K} \propto (a_{U,K})^3 / a_{\rm today}^3$ and the volume dilution behaves as $1/a^3 \propto T^3$, the volume factors alone contribute $(T_U/T_K)^3$. Residual annihilations after freeze out contribute a factor of order T_K/T_U for p-wave dominance. The most nontrivial aspect of the kination scenario is that since the freeze out condition is $\langle \sigma v \rangle n_\chi = m_\chi H/T$, with

$$H_K \sim \sqrt{\eta_\Phi} \left(\frac{T_K}{T_0} \right)^3 \frac{T_0^2}{M_{pl}} \tag{3.22}$$

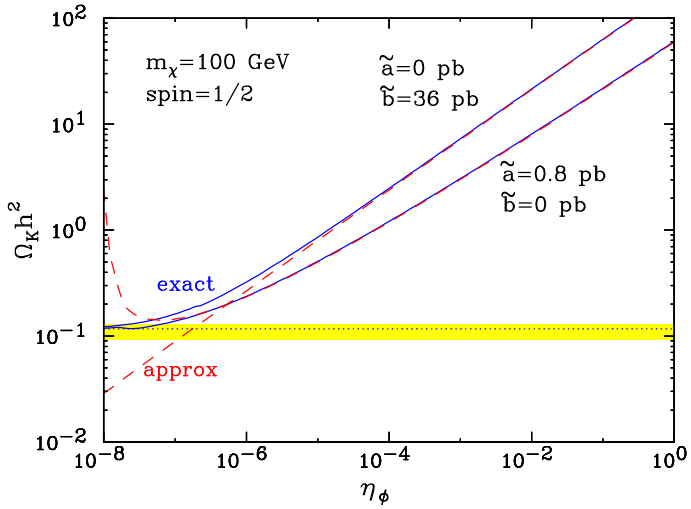

Figure 1: The dark matter relic abundance $\Omega_K h^2$ in the kination domination scenario, as a function of the kination parameter (3.4), for the case of a pure s-wave annihilator ($\tilde{a} = 0.8$ pb, $\tilde{b} = 0$) or a pure p-wave annihilator ($\tilde{a} = 0$, $\tilde{b} = 36$ pb) with spin 1/2 and mass $m_\chi = 100\,\mathrm{GeV}$. The (blue) solid lines give the exact result from eq. (3.14), while the (red) dashed lines correspond to the approximations (3.23) and (3.21). The horizontal dotted line and the (yellow) shaded band denote the current central value and 2σ range for the experimental determination of the dark matter relic abundance.

(recall $H^2 \propto \eta_\Phi/a^6$ during kination domination), $H_U \sim T_U^2/M_{pl}$, and $\langle\sigma v\rangle \propto T$ (p-wave dominance), there is a factor of T_K/T_0. Note that since $T_0/T_U \sim 10^{-3}$ and the difference between T_K and T_U is only logarithmically dependent on the $\dot{\Phi}^2$ energy density, it is unrealistic to obtain a ratio smaller than unity in eq. (3.21).

We similarly approximate eq. (3.14) in the limit of s-wave dominance to obtain

$$\frac{\Omega_K}{\Omega_U} \sim \frac{g_{*S}(T_U)}{g_{*S}(T_0)} \frac{T_U}{T_0} \frac{\sqrt{\eta_\Phi}}{\log(2u)\sqrt{g_*(T_U)}/2}. \tag{3.23}$$

Inserting typical numbers $\{m_\chi \sim 100$ GeV, $T_0 \sim 10^{-3}$ GeV, $g_{*S}(T_U) \sim g_*(T_K) \sim 10^2$, $g_{*S}(T_0) \approx 10.75$,$\tilde{b} = 5.4\times10^{-8}$ GeV^{-2}, $\eta_\Phi \sim 1\}$ into eq. (3.21) and eq. (3.23), we generically find for both cases

$$\frac{\Omega_K}{\Omega_U} \sim 10^3. \tag{3.24}$$

Hence, the kination scenario relic abundance is much larger than the usual freeze out scenario relic abundance for the same microphysical parameters governing the WIMP annihilation cross section. This is illustrated in figure 1, which shows the dark matter relic abundance $\Omega_K h^2$ in the kination domination scenario, as a function of the kination parameter (3.4), for the case of a pure s-wave annihilator ($\tilde{a} = 0.8$ pb, $\tilde{b} = 0$) or a pure p-wave annihilator ($\tilde{a} = 0$, $\tilde{b} = 36$ pb). We assume that the dark matter particle is a fermion with spin 1/2 and mass $m_\chi = 100\,\mathrm{GeV}$. The values for its annihilation cross-sections are chosen so that in the usual scenario ($\eta_\Phi = 0$) this particle would make up all of the dark matter, in agreement with the experimental determination of the dark matter relic abundance by

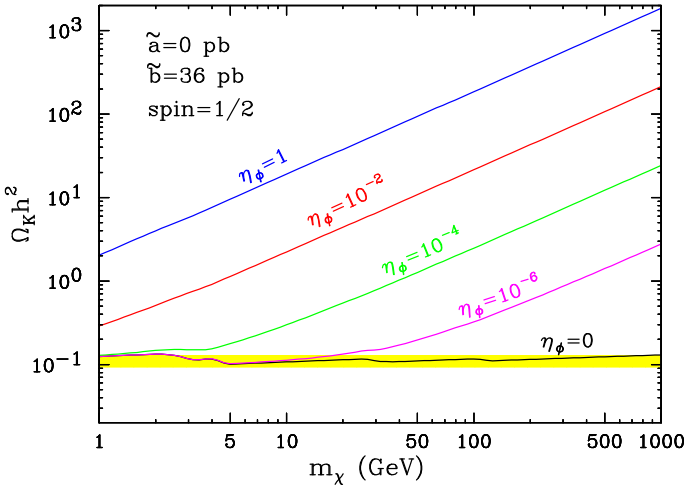

Figure 2: The dark matter relic abundance $\Omega_K h^2$ in the kination domination scenario, as a function of the mass m_χ of the dark matter particle, for the case of a pure p-wave annihilator ($\tilde{a} = 0$, $\tilde{b} = 36$ pb) and different values of the kination parameter η_Φ. The horizontal (yellow) shaded band denotes the current 2σ range for the experimental determination of the dark matter relic abundance.

WMAP and SDSS ($\Omega_\chi h^2 = 0.111^{+0.011}_{-0.015}$ at 2σ [1], as indicated by the horizontal dotted line and the (yellow) shaded band). The (blue) solid lines give the exact result from eq. (3.14), while the (red) dashed lines correspond to the approximations (3.23) and (3.21). We see that the approximate expressions work quite well, down to $\eta_\Phi \sim 10^{-7}$ for s-wave annihilators, and $\eta_\Phi \sim 10^{-5}$ for p-wave annihilators. While the approximations (3.23) and (3.21) are useful for understanding the scaling of the relic density in the presence of quintessence, in our numerical results below we shall always make use of the exact expression (3.14). From figure 1 we also see that, in agreement with the naive expectation (3.24), for $\eta_\Phi \sim 1$ and at this value of $m_\chi = 100\,\mathrm{GeV}$, kination domination provides an enhancement by about three orders of magnitude of the dark matter thermal relic density. The kination enhancement of the dark matter relic density can be even more pronounced, if the mass m_χ of the dark matter particle is larger, as evidenced in figure 2. There we plot the dark matter relic abundance $\Omega_K h^2$ in the kination domination scenario, this time as a function of the mass m_χ of the dark matter particle, for the case of a pure p-wave annihilator ($\tilde{a} = 0$, $\tilde{b} = 36$ pb) and different values of the kination parameter η_Φ. As in figure 1, the horizontal (yellow) shaded band denotes the current 2σ range for the experimental determination of the dark matter relic abundance. We see for example, that if the dark matter matter particle had a mass of order 1 TeV, kination may provide an enhancement of its relic density of up to 4 orders of magnitude!

Given these results, let us return to the issue of testing the WIMP hypothesis at colliders as discussed in section 2. To make the discussion more concrete, consider the following scenario. Suppose that colliders have found a WIMP of mass 100 GeV whose spin was measured to be 1/2. The lightest neutralino in supersymmetry is a standard such example. Furthermore, because of its Majorana nature, the neutralino typically annihilates predominantly in a p-wave, so $\tilde{a} \ll \tilde{b}$. The measurements of the neutralino couplings and

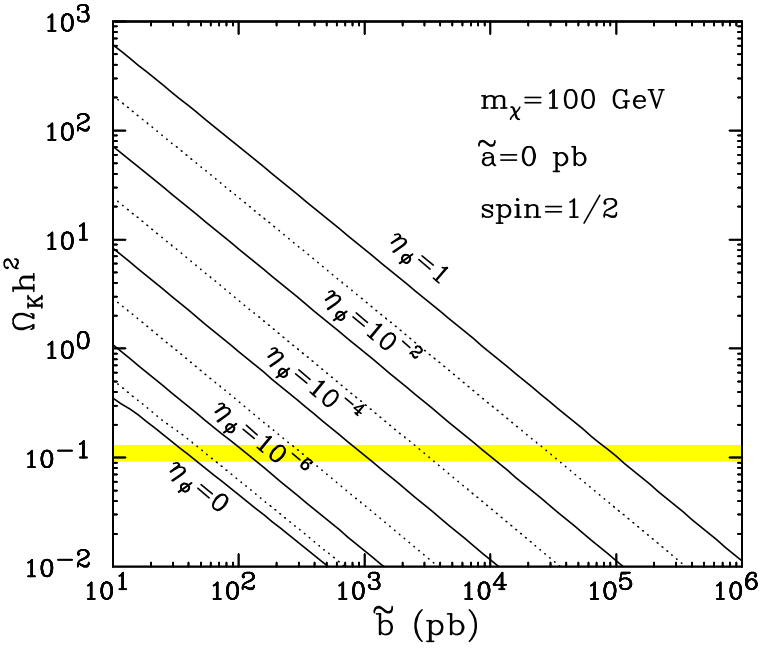

Figure 3: The dark matter relic abundance $\Omega_K h^2$ in the kination domination scenario, as a function of the annihilation cross-section $\tilde{b}$ of the dark matter particle, for the case of a pure p-wave annihilator ($\tilde{a} = 0$) of spin 1/2 and mass $m_\chi = 100\,\mathrm{GeV}$, for different values of the kination parameter η_Φ. The solid lines are plotted for η_Φ values as labelled on the plot (every other decade), while the dotted lines correspond to intermediate decades. The horizontal (yellow) shaded band denotes the current 2σ range for the experimental determination of the dark matter relic abundance.

the superpartner mass spectrum can then be translated into a bound on the annihilation cross-section σ_A, in this case its $\tilde{b}$ component. Given the bounds on $\tilde{b}$, one can then reconstruct the allowed range for the WIMP relic abundance, both with and without the effects of kination domination, as shown in figure 3. There we plot the dark matter relic abundance $\Omega_K h^2$ in the kination domination scenario, as a function of the annihilation cross-section $\tilde{b}$ of the dark matter particle, for different values of the kination parameter η_Φ. As in figures 1 and 2, the horizontal (yellow) shaded band denotes the current 2σ range for the experimental determination of the dark matter relic abundance. The prediction of standard cosmology (no kination domination) is given by the $\eta_\Phi = 0$ line.

As we alluded to earlier, the case which is especially interesting is the one where $\tilde{b}$ is determined to be *too large*, e.g. larger than, say, 100 pb, corresponding to outcome (2.3) in our discussion in the previous section.[3] Such a result can be interpreted in one of two ways. First, assuming standard cosmology, one can read off from the $\eta_\Phi = 0$ line the maximum fraction that such a WIMP can contribute to the dark matter budget of the Universe. Alternatively, assuming that the WIMP makes up 100% of the dark matter in the universe

[3]Indeed, other outcomes of the collider tests of the WIMP hypothesis, eqs. (2.1) and (2.2), would strongly disfavor the kination-dominated quintessence dark matter scenario and place an upper bound on the quintessence parameter η_Φ. Of course, quintessence die-hards may still argue that there are extra unseen annihilation channels into non-SM states. The corresponding increase in σ_A can be compensated by a nonzero value of η_Φ. While this is possible in principle, it would seem coincidental and rather fine-tuned.

JHEP10(2007)016

and following the horizontal shaded band, the lower bound on $\tilde{b}$ would imply a lower bound on η_Φ, i.e., a minimum value for the kinetic energy contribution of the quintessence field Φ to the total energy budget in the early universe. We would like to emphasize once again that the lower bound on $\tilde{b}$ would tend to be rather robust and difficult to invalidate - it would be derived based on some observed channel which would guarantee a minimum value for the WIMP annihilation rate.

4. Numerical results

In the previous section we have seen the possible interplay between dark matter and dark energy in the early universe. By now it is well appreciated that high-energy colliders offer the unique opportunity of creating and studying dark matter in the lab. Therefore, if there is a cosmological connection between dark matter and dark energy, high-energy colliders can also shed light on the nature of dark energy itself. We now analyze specific WIMP scenarios in the context of low energy supersymmetry, for which the LSP dark matter candidate is the lightest neutralino, to ascertain to what extent forthcoming and future collider experiments can probe dark energy and dark matter within this class of quintessence models of dark energy.

4.1 Choice of benchmark models

Hence, in the remainder of this section we shall use several study cases to investigate the capabilities of the LHC and ILC in determining the relevant dark matter and dark energy parameters. It has become customary to perform such studies, using specific "study points" in the parameter space of simple models. In particular, in case of supersymmetry, the model of choice has been "mSUGRA", as it has rather few input parameters. Three of them fix the values of the soft supersymmetry breaking parameters at the unification scale: the universal scalar mass m_0, the universal gaugino mass $M_{1/2}$, and the common trilinear term A_0. The remaining two mSUGRA model parameters are $\tan\beta$, the ratio of the Higgs vacuum expectation values, and the sign of the μ term in the superpotential. While the mSUGRA model is not representative of *every* possible incarnation of supersymmetry, it is nevertheless sufficiently general to exhibit four different regions in parameter space with a good dark matter candidate. Correspondingly, all of the recent sets of benchmark points suggested in the literature [62 – 64] have zeroed in on those regions, and proposed study points where the supersymmetric dark matter candidate (neutralino) makes up all of the dark matter in the universe.

In our case, we would like to include in our analysis the effect of kination, which, as we have already seen, tends to enhance the nominal prediction of the dark matter relic density. Therefore, the usual sets of mSUGRA benchmark points are ill suited for our purposes, if our goal is to provide a *measurement* of the kination parameter at colliders. Indeed, if the nominal calculation already yields a prediction in exact agreement with experiment, kination will then make things worse, and we can at best only place an upper limit on η_Φ. We have therefore chosen to modify the original set of LCC benchmark points of [18], so that the nominal calculation would yield a value for the relic density which

JHEP10(2007)016

is insufficient to explain all of the dark matter in the universe. Barring the existence of another, undiscovered yet dark matter candidate, the collider results could then be interpreted as measurements of η_Φ and would provide a non-trivial link between dark matter and dark energy. The values for the original LCC benchmark points (LCC1-LCC4) and our modified versions (LCC1′-LCC4′) are listed in table 1. The motivation behind each choice will be discussed in the following subsections. At this point we would only mention that we have tried to only minimally deviate from the original LCC points, and that in all but one case our point differs from its LCC counterpart in the value of a single mSUGRA parameter.

Previous studies have already estimated the expected accuracy with which high energy physics experiments can pinpoint the supersymmetry parameters at the original LCC benchmark points. One should keep in mind, however, that those estimates are only "best guesses" so far, and one would have a better idea of the actual precision only after the colliders have been operational for some time, which would allow for better understanding of the systematic uncertainties. Nevertheless, we can reliably estimate the collider precision for our LCC′ benchmarks. The LCC′ benchmark points yield rather large values for the WIMP annihilation rate, which is typically due to the dominance of a single channel: either an s-channel resonance or a coannihilation channel. Under those circumstances, it is important to know with great precision only the masses of the particles involved in the dominant channel, while the rest of the spectrum may remain rather uncertain, as long as it does not contribute significantly to the WIMP annihilation rate. In what follows, we shall therefore base our prediction for the collider precision in measuring the cosmological parameters, on the expected precision in measuring the masses of the particles entering the dominant annihilation channel. A more sophisticated analysis using the full information about the SUSY spectrum and utilizing Markov chain probabilistic techniques along the lines of [18] is beyond the scope of our paper, and will not, we believe, significantly change our conclusions.

4.2 LCC1′: a study point in the bulk region

In the remainder of this section we shall present our results for the expected accuracy in determining the dark matter properties at colliders. We shall first discuss the physics and the relevant measurements at each one of our benchmark points LCC1′-LCC4′. Our predictions for the expected allowed range in $\Omega_K h^2$ and η_Φ as determined by the LHC and ILC for each study point will be summarized in figure 9. The superpartner mass spectra for the four original LCC study points and for our modified LCC′ study points are listed in table 1.

The LCC1 study point was chosen in the bulk region, where the sleptons are relatively light, and neutralino annihilation proceeds predominantly through t-channel right-handed slepton exchange. At LCC1, there are 7 channels which contribute more than 1% to the annihilation rate, but the three dominant channels are $\tau^+\tau^-$ (32%) and $\mu^+\mu^-$ and e^+e^- (at 29% each). The remaining channels (neutrino pairs and $b\bar{b}$) are about 2% each. As one can see, the right-handed sleptons play the most important role in mediating neutralino annihilations – first, because they are the lightest sfermions in the spectrum, and second,

JHEP10(2007)016

	LCC1	LCC1′	LCC2	LCC2′	LCC3	LCC3′	LCC4	LCC4′
m_0	100	100	3280	3260	213	205	380	950
$M_{1/2}$	250	150	300	300	360	360	420	420
$\tan\beta$	10	10	10	10	40	40	53	50
A_0	-100	-100	0	0	0	0	0	0
sign(μ)	+1	+1	+1	+1	+1	+1	+1	-1
m_t	175	175	175	175	175	175	178	178
$\Omega_U h^2$	0.193	0.00127	0.106	0.0363	0.121	0.0329	0.104	0.0244
$\tilde{\chi}_1^0$	95.5	53.6	107.7	92.1	142.6	142.6	169.1	171.8
$\tilde{\chi}_2^0$	181.6	98.6	166.3	147.2	274.2	274.1	327.1	335.7
$\tilde{\chi}_3^0$	356.6	232.3	190.0	147.9	462.8	462.8	539.7	552.8
$\tilde{\chi}_4^0$	375.6	256.2	294.2	286.2	478.0	478.0	553.0	563.0
$\tilde{\chi}_1^+$	181.6	97.5	159.4	124.6	274.5	274.4	327.5	335.1
$\tilde{\chi}_2^+$	374.7	255.3	286.6	278.3	478.2	478.2	553.2	563.1
$\tilde{e}_R$	143.1	122.2	3277.3	3357.1	254.9	248.3	412.4	962.1
$\tilde{e}_L$	204.6	151.2	3280.1	3359.8	328.9	323.9	477.2	990.3
$\tilde{\nu}_e$	186.2	127.7	3276.4	3356.1	316.3	311.0	468.2	985.8
$\tilde{\tau}_1$	134.5	113.2	3251.6	3330.8	154.9	147.3	195.5	734.0
$\tilde{\tau}_2$	207.6	155.7	3267.7	3346.9	333.3	329.3	441.7	893.3
$\tilde{\nu}_\tau$	185.3	126.8	3263.8	3343.0	297.6	292.9	409.2	885.7
h	113.8	108.7	118.7	118.8	116.7	116.7	118.9	118.6
A	394.4	255.1	3242.2	3318.7	429.5	427.6	419.4	352.5
$\tilde{u}_R$	547.8	352.6	3311.0	3389.3	780.2	778.1	943.5	1274.9
$\tilde{u}_L$	564.4	360.4	3301.3	3380.1	805.0	802.9	971.3	1292.6
$\tilde{d}_R$	547.6	354.4	3313.4	3391.3	778.5	776.3	941.2	1273.6
$\tilde{d}_L$	570.4	369.7	3302.3	3381.0	809.3	807.2	974.8	1295.1
$\tilde{t}_1$	400.9	237.9	1976.1	2023.0	602.5	601.4	715.6	872.9
$\tilde{t}_2$	577.7	407.8	2719.9	2783.8	764.9	763.8	875.4	1009.0
$\tilde{b}_1$	514.3	327.4	2709.9	2773.6	691.0	689.5	795.1	950.8
$\tilde{b}_2$	538.7	348.8	3241.3	3318.3	743.0	741.5	861.8	1011.6
$\tilde{g}$	611.2	386.2	850.1	852.5	856.2	855.9	993.0	1027.5

Table 1: mSUGRA parameter sets for the four LCC study points and their variations used in this study. We also show the relic density and the superpartner spectrum (the masses are listed in units of GeV) predicted at each point as calculated with micrOMEGAs [65 – 67] and `ISAJET` version 7.69 [68].

because they have the largest hypercharge (the LSP is 97.4% Bino at this point and its couplings are proportional to hypercharge). Under those circumstances, in order to pinpoint the WIMP relic density, one has to measure precisely the masses of the right handed sleptons and the LSP, at the same time making sure that the remaining sparticles in the spectrum are relatively heavy. At the LHC, the slepton masses are difficult to measure in direct slepton production [69, 70], due to the relatively small slepton production cross-

section and large SM backgrounds. Fortunately, point LCC1 has relatively light colored superpartners (squarks and gluino) which can be produced abundantly at the LHC and in their cascade decays may yield sleptons indirectly. In particular, the decays of $\tilde{\chi}_2^0$ are predominantly to right-handed sleptons (since they are the only sfermions lighter than $\tilde{\chi}_2^0$). The measurements are by no means trivial, since one would have to extract the slepton and neutralino masses from a sufficient set of observed kinematic endpoints. However, the expectations are that one could measure the LSP mass to within 5% and the neutralino-slepton mass differences to within a few GeV (for more details, see [18]). Of course, since the sleptons at point LCC1 are within the kinematic reach of the ILC, their masses (as well as the LSP mass) can be determined at the per mil level at the ILC.

As we discussed earlier, our strategy will be to modify the original LCC benchmark points so that the resulting relic density is *too low* and can accommodate the kination dominated quintessence scenario. Notice that the relic density at point LCC1 is already too large[4] (almost double the WMAP value), which appears to make our job rather difficult. There are several ways to reduce the value of Ωh^2. For example, one could attempt to reduce the slepton masses even further. However, this will not help in our case — first, it will eventually take us into the coannihilation region discussed later on in section 4.4. Furthermore, the value of m_0 at point LCC1 is already small enough so that the slepton masses are dominated by the radiative corrections due to the gaugino terms in the RGE's. The slepton masses are therefore much more sensitive to the parameter $M_{1/2}$. This is why we choose to modify the LCC1 point by changing the value of $M_{1/2}$. The resulting variation in the relic density $\Omega_U h^2$ as calculated within standard cosmology, is shown in figure 4a, for fixed $m_0 = 100\,\text{GeV}$, $A_0 = -100\,\text{GeV}$, $\tan\beta = 10$, $\mu > 0$ and $m_t = 175\,\text{GeV}$. The horizontal (green) shaded band denotes the current 2σ range for the experimental determination of the dark matter relic abundance. The vertical (yellow) shaded band on the left is ruled out by the negative chargino searches at LEP. Since the parameter $M_{1/2}$ controls the values of the gaugino masses, when it becomes too small, there will be a light (wino-like) chargino in the spectrum. It should be kept in mind that the LEP bound on the chargino mass is also a function of the electron sneutrino mass $\tilde{\nu}_e$: the bound is diluted in the presence of a light sneutrino due to destructive interference between the Z/γ and $\tilde{\nu}_e$ mediated diagrams of chargino production. When moving in the opposite direction — increasing $M_{1/2}$ — we encounter a region where the lightest slepton ($\tilde{\tau}_1$) becomes increasingly lighter relative to the lightest neutralino ($\tilde{\chi}_1^0$) and eventually becomes the LSP in the region denoted by the vertical (yellow) shaded band on the right.

Figure 4a exhibits three regions where the relic abundance is reduced below the WMAP level. On the right-hand side, at large $M_{1/2}$ and near the stau LSP limit, this is due to stau coannihilations (see section 4.4). On the left-hand side, at low $M_{1/2}$, we see two dips in $\Omega_U h^2$ due to resonant neutralino annihilations through a Z (the left dip) and the light CP-even Higgs boson h (the right dip). The Z resonance is already inside the excluded region but the h resonance is still allowed. That is where we chose our modified LCC1$'$

[4]To some extent this is related to ensuring that the Higgs boson mass is above the LEP limit (we shall return to this point later on).

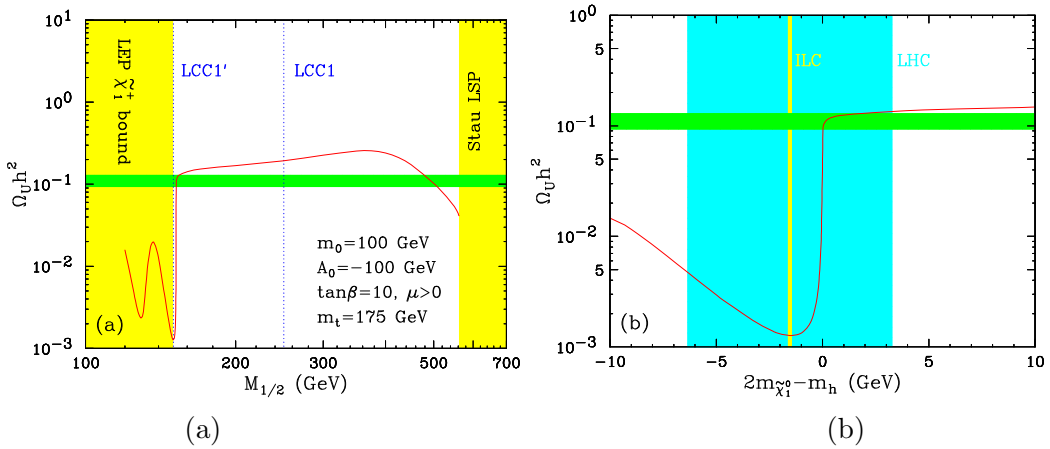

(a) (b)

Figure 4: a) The dark matter relic abundance $\Omega_U h^2$ in standard cosmology, as a function of the universal gaugino mass parameter $M_{1/2}$ in minimal supergravity, for fixed $m_0 = 100\,\text{GeV}$, $A_0 = -100\,\text{GeV}$, $\tan\beta = 10$, $\mu > 0$ and $m_t = 175\,\text{GeV}$. The horizontal (green) shaded band denotes the current 2σ range for the experimental determination of the dark matter relic abundance. The vertical (yellow) shaded band on the left is ruled out by the negative chargino searches at LEP. The other vertical (yellow) shaded band on the right is ruled out because the lightest superpartner (stau) is charged. The vertical line marked LCC1 (LCC1′) denotes the $M_{1/2}$ value for the LCC1 (LCC1′) study point (see table 1). b) The same as a), but plotted versus the mass difference $2m_{\tilde{\chi}_1^0} - m_h$, which indicates the proximity to the light Higgs pole. The vertical light blue (yellow) band indicates the expected experimental precision in determining the value of the combination $2m_{\tilde{\chi}_1^0} - m_h$ at the LHC (ILC).

point, marked by the vertical line labelled LCC1′.

The SUSY spectrum of point LCC1′ is given in table 1. It is somewhat lighter than the spectrum at LCC1, but the hierarchy of states is similar, which allows us to assume the same precision in the sparticle mass determinations as for point LCC1. The chargino mass is 97.5 GeV, but (as discussed above) is still allowed due to the presence of a light electron sneutrino, which degrades the LEP chargino bound. One might be worried that the light CP-even Higgs boson mass is also lighter - 108.7 GeV, which is below the LEP Higgs mass limit. Indeed such a light Higgs boson is ruled out. However, the exact value of the Higgs boson mass is not essential for our analysis, since we are only interested in the *precision* with which the masses can be determined, rather than their actual values. At the original point LCC1 the problem was avoided by considering a heavier spectrum, which resulted in an unacceptable value for the relic density. Both of these problems can be simply solved by relaxing some of the mSUGRA assumptions, for example, scalar mass nonuniversality in the third generation [71] can easily lift the Higgs mass, while gaugino non-universality can remove any remaining tension with the light chargino bound from LEP.

Given the SUSY spectrum of point LCC1′, we now turn our attention to the corresponding prediction for the WIMP relic density at colliders. The most important feature of our spectrum is that $2m_{\tilde{\chi}_1^0} \approx m_h$, which allows the neutralinos to annihilate very efficiently on the Higgs resonance. Unlike point LCC1, we now find that the dominant neutralino

JHEP10(2007)016

annihilation channels are $b\bar{b}$ (90%) and $\tau^+\tau^-$ (9%), as expected on the h resonance. This implies that the Higgs resonant diagram by far overwhelms all other neutralino annihilation processes *combined*. This can already be guessed from figure 4a, where the turn on of the resonant h diagram causes a sharp drop in the relic density of almost 2 orders of magnitude. The same effect is even more evident in figure 4b, where we plot our results from figure 4a versus the mass difference $2m_{\tilde{\chi}_1^0} - m_h$, which is an indicator of the proximity to the light Higgs pole. Figures 4a and 4b make it clear that in order to predict the neutralino relic abundance, we only need to concentrate on the precision with which the masses $m_{\tilde{\chi}_1^0}$ and m_h can be determined at colliders. At the LHC, m_h can be precisely measured in the diphoton channel, therefore the dominant uncertainty is still from the determination of $m_{\tilde{\chi}_1^0}$, which we take to be 5%, as for point LCC1. At the ILC, we take the uncertainty on both $m_{\tilde{\chi}_1^0}$ and m_h to be 0.05 GeV [18]. The resulting uncertainty on the combination $2m_{\tilde{\chi}_1^0} - m_h$ at the LHC (ILC) is shown in figure 4b by the light blue (yellow) band. The remaining mass spectrum measurements can be assumed to be similar to those for point LCC1, but as far as the relic density is concerned, they become largely irrelevant, their only significance being to show that we are sufficiently far away from other special regions, e.g. the stau coannihilation region.

Figure 4b can be used to directly translate the uncertainty on $2m_{\tilde{\chi}_1^0} - m_h$ into the corresponding uncertainty on $\Omega_U h^2$, as calculated in standard cosmology. Turning on the effect of kination dominance, we then find the result in figure 9a, which shows the expected precision in the simultaneous determination of the dark matter relic abundance $\Omega_K h^2$ and quintessence parameter η_Φ at the LHC (blue band) and the ILC (red band). Figure 9a illustrates our main point — that in kination dominated quintessence scenarios, colliders constrain *a combination* of the dark matter and dark energy properties. In the case of point LCC1′, measurements at the LHC alone will still be consistent with a WIMP hypothesis within standard cosmology. One would really need the precision of the ILC in order to see that within standard cosmology, this particular WIMP is not enough to explain all of the dark matter. Alternatively, if the WIMP does make all of the dark matter in the universe, the ILC, combined with precision cosmology, provide a measurement of the quintessence parameter η_Φ at the percent level.

4.3 LCC2′: a study point in the focus point region

In this and the next two subsections, we shall repeat the analysis we have just done for the LCC1′ bulk point, for our other three study points. Study points in the bulk region of mSUGRA are relatively "collider-friendly", in the sense that a relatively large number of particles can be produced and studied, and as a result, a multitude of measurements can be made. The remaining three study points are chosen in regions where typically a smaller set of states is accessible at colliders. Nevertheless, one can still obtain a similar precision on the relic density determination, since the limited knowledge of the spectrum is partially offset by the fact that only a few channels dominate the annihilation rate, and often it is only a specific feature of the spectrum which governs the annihilation rate and thus needs to be known precisely.

JHEP10(2007)016

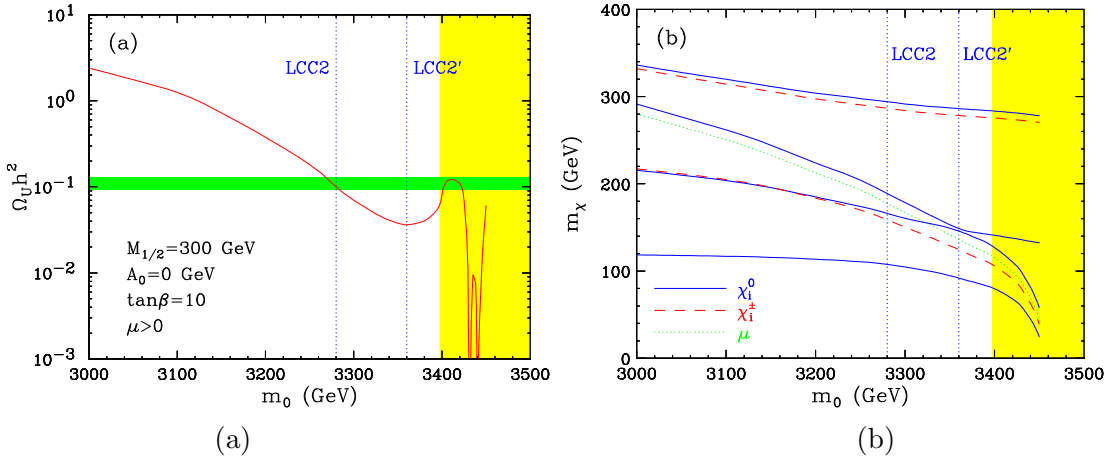

Figure 5: a) The dark matter relic abundance $\Omega_U h^2$ in standard cosmology, as a function of the universal scalar mass parameter m_0 in minimal supergravity, for fixed $M_{1/2} = 300\,\text{GeV}$, $A_0 = 0\,\text{GeV}$, $\tan\beta = 10$, $\mu > 0$ and $m_t = 175\,\text{GeV}$. The horizontal (green) shaded band denotes the current 2σ range for the experimental determination of the dark matter relic abundance. The vertical (yellow) shaded band on the right is ruled out from the negative chargino searches at LEP. The vertical line marked LCC2 (LCC2′) denotes the m_0 value for the LCC2 (LCC2′) study point (see table 1). b) The masses of the charginos (dashed, red) and neutralinos (solid, blue), and the value of the μ parameter (dotted, green) as a function of m_0, for the same fixed parameters as in a).

The LCC2 study point was chosen in the so called "focus point" region of mSUGRA [72, 73]. The region is characterized by relatively heavy scalars, which alleviates the tension with a number of phenomenological constraints: e.g. flavor problem, CP-violation, light Higgs boson mass, proton decay etc. [74 – 76]. The LSP in the focus point region is still predominantly Bino, but has a non-negligible Higgsino component, which opens up new annihilation channels into gauge and/or Higgs bosons [77]. For example, at LCC2 the LSP is 68% Bino, 28% Higgsino, and 4% Wino, and the dominant annihilation channels are W^+W^- (78%), ZZ (12%) and Zh (6%). The prediction of the relic density in this region is perhaps most sensitive to the amount of gaugino-higgsino mixing: increasing (decreasing) the Higgsino component of the LSP decreases (increases) the relic abundance. This is illustrated in figure 5a, where we show the dark matter relic abundance $\Omega_U h^2$ in standard cosmology as a function of the universal scalar mass parameter m_0, for fixed $M_{1/2} = 300\,\text{GeV}$, $A_0 = 0\,\text{GeV}$, $\tan\beta = 10$, $\mu > 0$ and $m_t = 175\,\text{GeV}$. As before, the horizontal (green) shaded band denotes the current 2σ range for the experimental determination of the dark matter relic abundance. The value of the Higgsino mass parameter μ is anti-correlated with m_0, as seen in figure 5b, where we show the masses of the charginos (dashed, red) and neutralinos (solid, blue), and the value of the μ parameter (dotted, green) as a function of m_0, for the same fixed parameters as in figure 5a. We see that increasing the value of m_0 away from the LCC2 point will lead to a smaller μ, larger Higgsino component in the LSP, and correspondingly a lower $\Omega_U h^2$. This is the motivation behind our choice of the new value of $m_0 = 3360\,\text{GeV}$ for our modified study point LCC2′, as marked by the

JHEP10(2007)016

vertical line in figures 5a and 5b. At point LCC2′, the LSP is well mixed: 56% Higgsino, 38% Bino and 6% Wino. The dominant annihilation channels are still W^+W^- (88%) and ZZ (5%). If we increase m_0 even further, the LSP becomes purely Higgsino-like, and its mass begins to track the decreasing value of μ, eventually closing the W^+W^- and ZZ annihilation channels, which leads to the local increase in $\Omega_U h^2$ observed in figure 5a. While this increase is in principle sufficient to bring the prediction for $\Omega_U h^2$ back to the desired level, it takes place inside a region of parameter space (shaded in yellow in figure 5) where the lightest (Higgsino-like) chargino is too light and is ruled out by LEP.[5] Just as in figure 4a, inside the light chargino region we again find two sharp dips in $\Omega_U h^2$, which correspond to resonant annihilations on the h and Z pole, respectively.

Points LCC2 and LCC2′ have similar spectra. The sfermions are very heavy and will escape detection at the LHC and ILC. Gluino production at the LHC will lead to long decay chains yielding jets, leptons and missing energy. B-tagging can improve the sensitivity of the gluino search [79] and allow for a gluino mass measurement at the LHC [80]. However, in the focus point region, the relic density is determined primarily by the properties of the neutralino and chargino sectors, which will be mapped out relatively well at the ILC [12, 81, 82]. In particular, all but the heaviest chargino and neutralino states are accessible to the ILC at a center-of-mass energy of 500 GeV. Given the expected set of measurements available at point LCC2 [81, 18] estimates the resulting uncertainty in $\Omega_U h^2$ as 82% at the LHC and 14% at the ILC. Given that the SUSY spectrum at our point LCC2′ has only minor quantitative differences from the spectrum at LCC2, we expect a similar precision on $\Omega_U h^2$ at point LCC2′ as well. Using the same uncertainty levels (82% at LHC and 14% at ILC), we show in figure 9b the resulting expectations for the simultaneous determination of the dark matter relic abundance $\Omega_K h^2$ and quintessence parameter η_Φ at point LCC2′ for the LHC (blue band) and the ILC (red band). Our result should be taken with a grain of salt, since we have not done a dedicated analysis of the spectroscopy measurements at point LCC2′. Nevertheless, it seems that already at the LHC one would be able to place a lower bound on the quintessence parameter η_Φ, and limit its value to within 2-3 orders of magnitude. The ILC, in turn, will significantly narrow down the allowed range for η_Φ and within the context of our scenario, provide a unique probe of dark energy, unavailable by other means.

4.4 LCC3′: a study point in the stau coannihilation region

In most of the mSUGRA parameter space, the LSP is sufficiently lighter than the rest of the SUSY spectrum, so that the relic density is determined primarily by the LSP self-annihilation rate. However, mSUGRA also exhibits special regions where the LSP is sufficiently degenerate with another supersymmetric particle, so that both are present at freeze out and can affect the resulting dark matter relic density both through their self-annihilations as well as their co-annihilations with each other. In general, turning on coannihilations can lead to an increase or a decrease of the relic density, depending on

[5] The chargino constraint can be evaded for larger values of m_0 and $M_{1/2}$, where the pure Higgsino LSP can become a viable dark matter candidate [78].

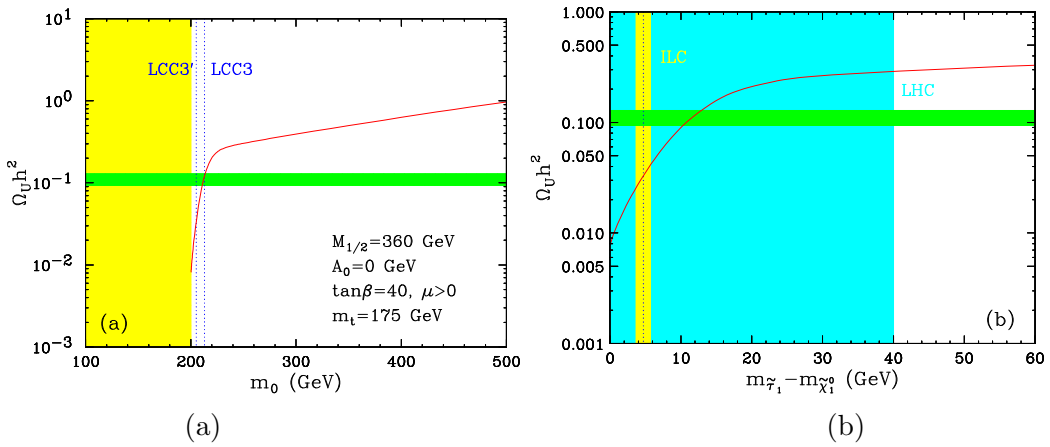

(a) (b)

Figure 6: a) The dark matter relic abundance $\Omega_U h^2$ in standard cosmology, as a function of the universal scalar mass parameter m_0 in minimal supergravity, for fixed $M_{1/2} = 360\,\text{GeV}$, $A_0 = 0\,\text{GeV}$, $\tan\beta = 40$, $\mu > 0$ and $m_t = 175\,\text{GeV}$. The horizontal (green) shaded band denotes the current 2σ range for the experimental determination of the dark matter relic abundance. The vertical (yellow) shaded band on the left is ruled out because the lightest superpartner (stau) is charged. The vertical line marked LCC3 (LCC3′) denotes the m_0 value for the LCC3 (LCC3′) study point (see table 1). b) The same as a), but plotted versus the mass difference $m_{\tilde{\tau}_1} - m_{\tilde{\chi}_1^0}$, which controls the effect of stau coannihilations. The vertical light blue (yellow) band indicates the expected experimental precision in determining the value of the mass splitting $m_{\tilde{\tau}_1} - m_{\tilde{\chi}_1^0}$ at the LHC (ILC).

the type and properties of the coannihilating particle. In mSUGRA the LSP is usually a Bino-like neutralino, whose self-annihilation rates are typically rather small, overclosing the universe. The presence of coannihilations would then typically tend to enhance the overall effective annihilation rate and lower the dark matter relic abundance.

Point LCC3 was chosen in the region where the lightest neutralino is very close in mass to the lightest tau slepton $\tilde{\tau}_1$ (see table 1). Their mass splitting was carefully adjusted so that the neutralino-stau coannihilations [83] would dilute the relic density precisely to the WMAP levels. In addition to the usual neutralino annihilation channels $\tilde{\chi}_1^0\tilde{\chi}_1^0 \to b\bar{b}$ (21%), $\tilde{\chi}_1^0\tilde{\chi}_1^0 \to \tau^+\tau^-$ (12%), $\tilde{\chi}_1^0\tilde{\chi}_1^0 \to \mu^+\mu^-$ and $\tilde{\chi}_1^0\tilde{\chi}_1^0 \to e^+e^-$ (5% each); we also have sizable coannihilation effects: $\tilde{\chi}_1^0\tilde{\tau}_1 \to h\tau$ (21%), $\tilde{\chi}_1^0\tilde{\tau}_1 \to \gamma\tau$ (17%) and $\tilde{\chi}_1^0\tilde{\tau}_1 \to Z\tau$ (6%). Naturally, reducing the neutralino-stau mass splitting even further would enhance the coannihilation contribution, and drop $\Omega_U h^2$ below WMAP levels, which is what we need for our modified study point. A simple way to control the $\tilde{\chi}_1^0$-$\tilde{\tau}_1$ mass splitting is provided by the parameter m_0 which affects the mass of $\tilde{\tau}_1$, but not $\tilde{\chi}_1^0$. This is illustrated in figure 6a where we show the dark matter relic abundance $\Omega_U h^2$ in standard cosmology, as a function of the universal scalar mass parameter m_0 in minimal supergravity, for fixed $M_{1/2} = 360\,\text{GeV}$, $A_0 = 0\,\text{GeV}$, $\tan\beta = 40$, $\mu > 0$ and $m_t = 175\,\text{GeV}$. The horizontal (green) shaded band denotes the current 2σ range for the experimental determination of the dark matter relic abundance. The vertical line marked LCC3 (LCC3′) denotes the m_0 value for the LCC3 (LCC3′) study point (see table 1). The value of m_0 cannot be too low, since then $\tilde{\tau}_1$ becomes the LSP (in the vertical yellow-shaded band). Nevertheless,

JHEP10(2007)016

close to the charged LSP region, the relic density gets to about an order of magnitude below the WMAP preferred value. At point LCC3′, the neutralino-stau mass splitting is reduced from 12.3 GeV down to 4.7 GeV. This is sufficient to make coannihilations and stau annihilations dominate the relic density calculation. At point LCC3′ we find that $\tilde{\chi}_1^0\tilde{\chi}_1^0$ annihilation processes only account for about 6% of the total annihilation rate. The dominant channels for dark matter number-changing processes are $\tilde{\chi}_1^0\tilde{\tau}_1 \to h\tau$ (25%), $\tilde{\chi}_1^0\tilde{\tau}_1 \to \gamma\tau$ (17%), $\tilde{\tau}_1^+\tilde{\tau}_1^- \to hh$ (17%), $\tilde{\tau}_1^+\tilde{\tau}_1^- \to \tau^+\tau^-$ (11%), etc.

Precision spectroscopy at points LCC3 and LCC3′ is rather challenging at the LHC. For one, the leptonic decay chain $\tilde{\chi}_2^0 \to \ell^+\ell^-\tilde{\chi}_1^0$ is lost, as $\tilde{\chi}_2^0$ predominantly decays to taus. Furthermore, because of the small $\tilde{\chi}_1^0$-$\tilde{\tau}_1$ mass splitting, the taus from the $\tilde{\tau}_1$ decay tend to be relatively soft and difficult to reconstruct. A couple of recent analyses have attempted simultaneous extraction of the neutralino-stau mass difference and the gluino mass in a channel with jets, 2τ's and missing energy [84] or a channel with jets, 3τ's plus missing energy [85]. However, it was found that those methods fail at very low neutralino-stau mass differences — below 5 GeV, as is the case of our point LCC3′. We shall therefore conservatively assume that in the absence of a definitive measurement, the LHC can only rule out large enough mass splittings (~ 40 GeV) which would have made a measurement possible. The ILC, on the other hand, can measure a neutralino-stau mass splitting as low as 5 GeV, down to about ± 1 GeV [86, 87]. These uncertainties are used in figure 6b, where we plot the result from figure 6a versus the mass difference $m_{\tilde{\tau}_1} - m_{\tilde{\chi}_1^0}$, which controls the effect of stau coannihilations. The vertical light blue (yellow) band indicates the expected experimental precision in determining the value of the mass splitting $m_{\tilde{\tau}_1} - m_{\tilde{\chi}_1^0}$ at the LHC (ILC), as discussed above. We can now use the result from figure 6b to anticipate the precision (shown in figure 9c) in the simultaneous determination of the dark matter relic abundance $\Omega_K h^2$ and quintessence parameter η_Φ at point LCC3′, for the case of the LHC (blue band) and the ILC (red band). The challenges at the LHC mentioned earlier are readily evident, as the LHC results alone will still be consistent with standard cosmology, ruling out only the largest possible values of η_Φ. With the addition of the ILC, one is again able to pinpoint quite accurately the quintessence parameter, and rule out the WIMP scenario within standard cosmology.

4.5 LCC4′: a study point in the Higgs funnel region

Our final example is a study point illustrating the so called "Higgs funnel" case [88, 89]. The SUSY spectrum at point LCC4 is somewhat similar to the one at point LCC3, however, the relic density is controlled by a different physics process. Here neutralino annihilations occur sufficiently close to the A resonance, so that the relevant parameters are the heavy Higgs masses and widths. In this sense, the situation is similar to our modified "bulk" point studied in section 4.2, where neutralinos annihilated near the light Higgs pole.

When neutralino annihilations occur exactly on the A pole, the relic density is typically too low, since the annihilation cross-sections are suppressed only by the Higgs width instead of the Higgs mass. Conversely, when neutralinos annihilate far away from the resonant pole, the relic density is determined by the other annihilation channels and is typically too large (unless we are in one of the regions discussed in the previous three sections). Therefore,

JHEP10(2007)016

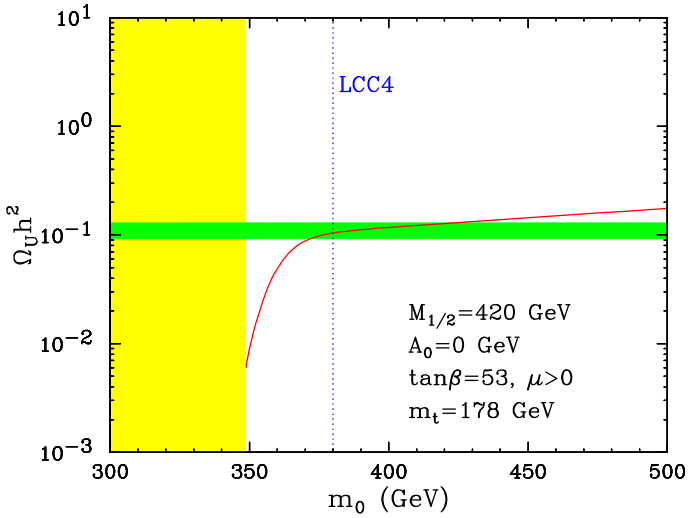

Figure 7: The dark matter relic abundance $\Omega_U h^2$ in standard cosmology, as a function of the universal scalar mass parameter m_0 in minimal supergravity, for fixed $M_{1/2} = 420\,\text{GeV}$, $A_0 = 0\,\text{GeV}$, $\tan\beta = 53$, $\mu > 0$ and $m_t = 178\,\text{GeV}$. The horizontal (green) shaded band denotes the current 2σ range for the experimental determination of the dark matter relic abundance. The vertical (yellow) shaded band on the left is ruled out because the lightest superpartner (stau) is charged. The vertical line marked LCC4 denotes the m_0 value for the LCC4 study point (see table 1).

there are two special places, on *both* sides of the A pole, where the relic density will be just right. The parameters for point LCC4 were chosen so that neutralino annihilations take place in the right place below the A resonance. The dominant annihilation channels at point LCC4 are $\tilde{\chi}_1^0\tilde{\chi}_1^0 \to b\bar{b}$ (78%) and $\tilde{\chi}_1^0\tilde{\chi}_1^0 \to \tau^+\tau^-$ (14%), indicative of the heavy Higgs branching fractions into fermion pairs.

Following our usual procedure, we wish to modify the LCC4 point so that to reduce the relic abundance. Since we are already in the vicinity of the A pole, the simplest way to achieve this without leaving the funnel region, is to simply reduce the heavy Higgs masses so that neutralino annihilations proceed on resonance. In mSUGRA, the Higgs masses are directly controlled by the m_0 parameter and therefore can be reduced by lowering m_0. Figure 7 shows the resulting variation of the dark matter relic abundance $\Omega_U h^2$ in standard cosmology, for fixed values of the remaining LCC4 parameters ($M_{1/2} = 420\,\text{GeV}$, $A_0 = 0\,\text{GeV}$, $\tan\beta = 53$, $\mu > 0$ and $m_t = 178\,\text{GeV}$). As usual, the horizontal (green) shaded band denotes the current 2σ range for the experimental determination of the dark matter relic abundance. The vertical line marked LCC4 denotes the m_0 value for the LCC4 study point (see table 1). One might attribute the observed sharp reduction in the relic density at lower m_0 to approaching the heavy Higgs pole, however this is not really the case. In the vertical (yellow) shaded band on the left we find a stau LSP, hence this region is cosmologically ruled out. Furthermore, near its boundary the neutralino and stau are quite degenerate, and we encounter the stau coannihilation situation discussed in section 4.4. We have checked that the reduction in $\Omega_U h^2$ near the stau LSP boundary is primarily due to stau coannihilations as opposed to resonant annihilations on the Higgs pole

JHEP10(2007)016

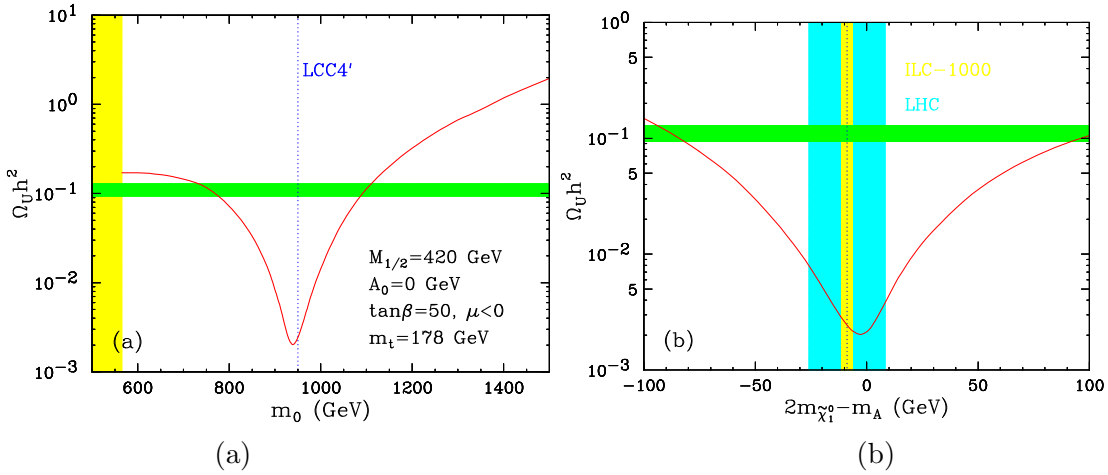

(a) (b)

Figure 8: a) The dark matter relic abundance $\Omega_U h^2$ in standard cosmology, as a function of the universal scalar mass parameter m_0 in minimal supergravity, for fixed $M_{1/2} = 420\,\text{GeV}$, $A_0 = 0\,\text{GeV}$, $\tan\beta = 50$, $\mu < 0$ and $m_t = 178\,\text{GeV}$. The horizontal (green) shaded band denotes the current 2σ range for the experimental determination of the dark matter relic abundance. The vertical (yellow) shaded band on the left is ruled out because there is a very light Higgs boson in the spectrum. The vertical line marked LCC4′ denotes the m_0 value for the LCC4′ study point (see table 1). b) The same as a), but plotted versus the mass combination $2m_{\tilde{\chi}_1^0} - m_A$, which indicates the proximity to the heavy Higgs pole. The vertical light blue (yellow) band indicates the expected experimental precision in determining the value of the combination $2m_{\tilde{\chi}_1^0} - m_A$ at the LHC (ILC-1000).

(on the stau LSP boundary we still find $m_A - 2m_{\tilde{\chi}_1^0} \sim 75$ GeV). Therefore, the m_0 variation in the vicinity of the LCC4 study point does not reveal the classic two-sided funnel shape, since the other half of the funnel is obscured by the stau coannihilation region. Similar conclusions hold if we vary $\tan\beta$ instead - just like m_0, $\tan\beta$ affects in a similar way both the Higgs and stau masses. We therefore choose to select our point in a funnel region which is sufficiently far away from the stau coannihilation boundary. This can be simply achieved by switching the sign of the μ parameter, which reverses the sign of the $\tan\beta$ enhanced Yukawa coupling corrections, leading to larger stau masses relative to the heavy Higgs masses. We therefore modify the values of two parameters ($\tan\beta = 50$ and $\mu < 0$) and in figure 8a once again we show the variation of the dark matter relic abundance $\Omega_U h^2$ in standard cosmology, as a function of the universal scalar mass parameter m_0 in minimal supergravity. We now clearly observe the classic Higgs funnel shape. The minimum of the relic density is found right on resonance, around $m_0 = 940\,\text{GeV}$, and the WMAP values (shown by the horizontal green shaded band) can be achieved on either side. The stau LSP region is now sufficiently far away — in fact the vertical yellow-shaded region on the left in figure 8a is now ruled out because of a light Higgs boson in the spectrum. For our modified study point we choose the value $m_0 = 950\,\text{GeV}$ (denoted by the vertical blue line) where we similarly find the dominant annihilation channels to be $\tilde{\chi}_1^0\tilde{\chi}_1^0 \to b\bar{b}$ (91%) and $\tilde{\chi}_1^0\tilde{\chi}_1^0 \to \tau^+\tau^-$ (9%).

We are now in position to discuss our expectations for the precision of the dark matter

JHEP10(2007)016

and dark energy determinations at the LHC and ILC at point LCC4′. As with any such Higgs funnel point, it is most important to measure the heavy Higgs spectrum in addition to the LSP mass. For consistency, we shall again use the assumptions of [18], that at point LCC4 the LHC will be able to determine the neutralino (heavy Higgs) mass to within 17 GeV (1.5 GeV). Clearly, the error on the relevant mass combination $2m_{\tilde{\chi}_1^0} - m_A$ is then dominated by the error on the LSP mass determination. Therefore, we can use the same error estimates for our modified point LCC4′, which has a very similar value of the LSP mass. In figure 8b we again plot the dark matter relic abundance, for the same fixed parameters as in figure 8a, but this time versus the relevant mass combination $2m_{\tilde{\chi}_1^0} - m_A$ (compare to figure 4b). The vertical light blue band indicates the expected experimental precision in determining the value of the combination $2m_{\tilde{\chi}_1^0} - m_A$ at the LHC. Unfortunately, at both point LCC4 and LCC4′ the heavy Higgs spectrum is too heavy to be observed by the ILC at center-of-mass energy of 500 GeV (ILC-500). In addition, at our modified point LCC4′ the staus are also heavy enough to escape detection at the ILC-500. Since ILC-500 does not add anything new to the dark matter determinations, following [18] we choose to consider the ILC upgrade at center-of-mass energy of 1000 GeV (ILC-1000). There the chargino-neutralino sector becomes accessible and the LSP mass is expected to be measured to within 1.4 GeV. The vertical yellow band in figure 8b then indicates the corresponding experimental precision at ILC-1000 in determining the value of the combination $2m_{\tilde{\chi}_1^0} - m_A$ at our modified point LCC4′.

The experimental precision in determining the relevant sparticle properties from figure 8b can now easily be translated into the corresponding uncertainties on the dark matter and dark energy properties. The result for our modified point LCC4′ is shown in figure 9d. We see that, as in the case of LCC2′, the LHC can already uncover the mismatch between the measured WIMP particle properties and those required by standard cosmology. The LHC can also provide a surprisingly good determination of the kination parameter η_Φ – in fact, as can be seen by comparing the thickness of the LHC bands in the four panels of figure 9, point LCC4′ is where the LHC does the best job. The advantage of the ILC as a precision machine is also readily seen in all 4 panels. For point LCC4′ where the ILC-500 energy is not sufficient, it should be kept in mind that the ILC project will go ahead only after the first LHC results become available. Once the LHC observes the A resonance near 350 GeV, and indicates that all electroweak and colored superpartners are rather heavy, it would be clear that the ILC design effort would shift towards the higher energy ILC option.

5. Discussion and conclusions

We are entering a new era in which the discovery of new fundamental physics at colliders may help us answer some of the most important puzzles of cosmology. In particular, as the LHC is likely to lead to the discovery of WIMPs that are identical to the particles which make up dark matter galactic halos, we may soon learn about new microphysics which governs the evolution of the universe. Therefore, it is natural to ask which aspects of cosmology can be probed by the anticipated identification and microphysics of the dark matter particles.

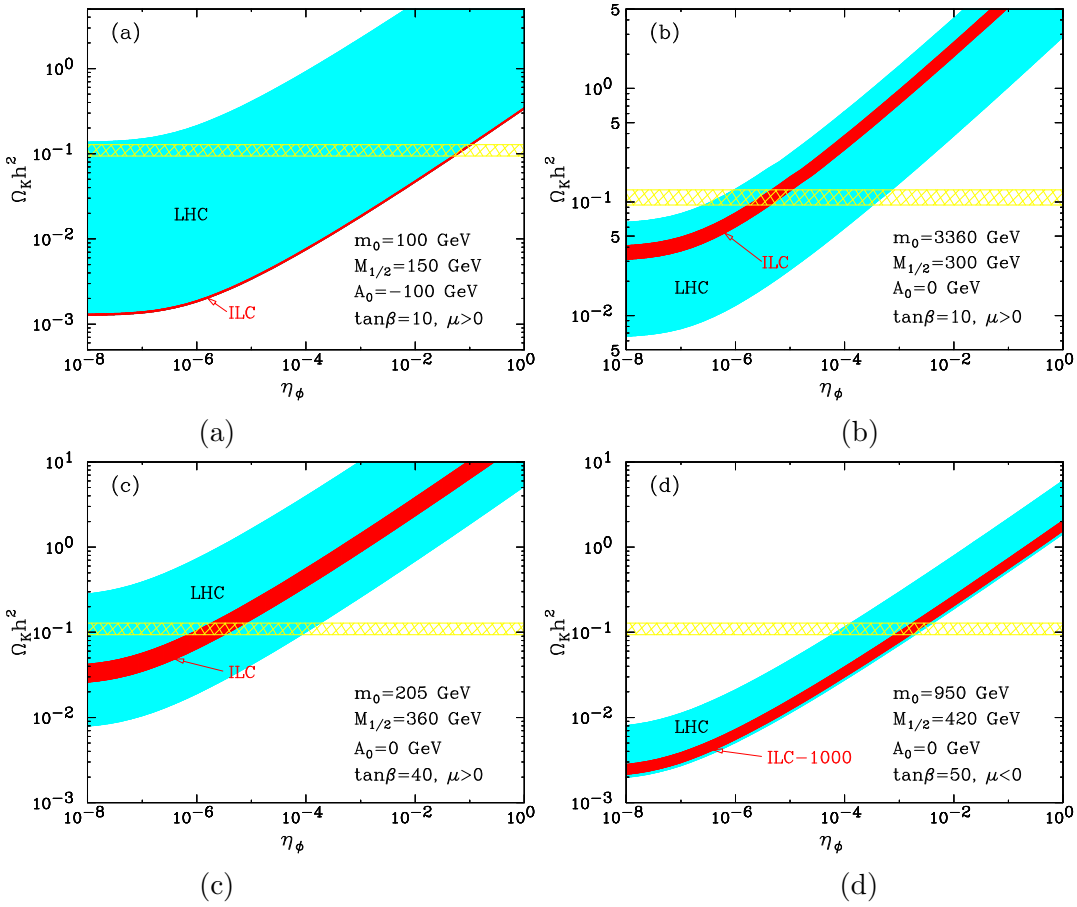

Figure 9: Expected precision in the simultaneous determination of the dark matter relic abundance $\Omega_K h^2$ and quintessence parameter η_Φ at the LHC (blue band) and the ILC (red band), for a) LCC1′, b) LCC2′, c) LCC3′ and d) LCC4′ study point.

One answer is that colliders will probe the period of our history at temperatures of order of a few GeV when the dark matter particles (assuming they are thermal WIMPs) presumably fell out of chemical thermal equilibrium. Therefore, we may be able to use collider information to probe properties of every significant energy component in the universe at the WIMP freeze out temperature, including field degrees of freedom such as quintessence, which may be responsible for the dark energy today. Since quintessence cannot be directly probed at any foreseeable terrestrial controlled experiments, we have investigated to what extent LHC and ILC can probe the cosmological properties of a very broad class of quintessence models parameterized by a single parameter $\eta_\Phi \lesssim 1$ (the ratio of energy density of quintessence to photon energy density at the time of BBN defined as $T = 1\,\mathrm{MeV}$), assuming that there was a period of kination domination during the time of freeze out.[6]

[6]A period of kination domination during which the scalar field energy density dilutes as a^{-6} is natural for $\eta_\Phi \sim \mathcal{O}(1)$ because of BBN constraints. The particular parametrization assumes that kination domination

JHEP10(2007)016

To compare the power of LHC and ILC in probing the early universe dark energy cosmology, we have considered mSUGRA models with parameters analogous to the set of four LCC study points [18] which were chosen to represent the four "good" dark matter regions. We find that for the cases in which the dark matter annihilates primarily through the lightest Higgs resonance and for the stau coannihilation region, the LHC is only able to put an upper bound on the parameter η_Φ characterizing the quintessence dynamics, while the ILC can put both an upper and a lower bound on η_Φ. Since a lower bound means a discovery of nontrivial dark energy dynamics while an upper bound is consistent with no dark energy component, the ILC has the potential to find supporting evidence for the possible kination history of dark energy. Indeed, it is remarkable that in the coannihilation region, the ILC can measure η_Φ as small as 10^{-6}, while the LHC can only put an upper bound of 10^{-4} on the same quantity. This should serve as yet one more important motivation for the construction of the ILC.

Furthermore, such conjectures about the underlying dark energy dynamics have other independent observable signatures which can be tested by near-future non-collider experiments. For example, observable signatures and correlated constraints were discussed in a previous publication [56] for the broad class of kination-dominated quintessence scenarios with an embedding in inflationary cosmology relevant for our present study. Therefore, just as big-bang nucleosynthesis has served as a sturdy pillar of cosmology to constrain dynamics of many conjectures of physics beyond the Standard Model, the anticipated identification of dark matter at colliders and astrophysics experiments will provide another robust pillar for cosmology, which will have profound consequences for uncovering the elusive nature of dark energy.

Acknowledgments

We would like to thank G. Kane for helpful conversations. The work of DJHC was supported by DOE Outstanding Junior Investigator Program through Grant No. DE-FG02-95ER40896. The work of KTM was supported by DOE Outstanding Junior Investigator Program through Grant No. DE-FG02-97ER41029. Fermilab is operated by Fermi Research Alliance, LLC under Contract No. DE-AC02-07CH11359 with the Department of Energy.

References

[1] WMAP collaboration, D.N. Spergel et al., *Wilkinson Microwave Anisotropy Probe (WMAP) three year results: implications for cosmology*, *Astrophys. J. Suppl.* **170** (2007) 377 [astro-ph/0603449].

[2] The SNLS collaboration, P. Astier et al., *The SuperNova Legacy Survey: measurement of Ω_M, Ω_Λ and w from the first year data set*, *Astron. Astrophys.* **447** (2006) 31 [astro-ph/0510447].

continues until temperatures of 1 MeV, but the results can be applied even to models for which this does not occur by making a model-dependent rescaling of the results.

[3] SDSS collaboration, D.J. Eisenstein et al., *Detection of the baryon acoustic peak in the large-scale correlation function of SDSS luminous red galaxies*, *Astrophys. J.* **633** (2005) 560 [astro-ph/0501171].

[4] Supernova Search Team collaboration, A.G. Riess et al., *Type IA supernova discoveries at $z > 1$ from the Hubble space telescope: evidence for past deceleration and constraints on dark energy evolution*, *Astrophys. J.* **607** (2004) 665 [astro-ph/0402512].

[5] G. Polesello and D.R. Tovey, *Constraining SUSY dark matter with the ATLAS detector at the LHC*, *JHEP* **05** (2004) 071 [hep-ph/0403047].

[6] M. Battaglia, I. Hinchliffe and D. Tovey, *Cold dark matter and the LHC*, *J. Phys.* **G 30** (2004) 217 [hep-ph/0406147].

[7] B.C. Allanach, G. Belanger, F. Boudjema and A. Pukhov, *Requirements on collider data to match the precision of WMAP on supersymmetric dark matter*, *JHEP* **12** (2004) 020 [hep-ph/0410091].

[8] M. Battaglia, *Study of dark matter inspired CMSSM scenarios at a TeV-class linear collider*, hep-ph/0410123.

[9] R.R. de Austri, R. Trotta and L. Roszkowski, *A Markov chain Monte Carlo analysis of the CMSSM*, *JHEP* **05** (2006) 002 [hep-ph/0602028].

[10] J.L. Bourjaily and G.L. Kane, *What is the cosmological significance of a discovery of wimps at colliders or in direct experiments?*, hep-ph/0501262.

[11] G. Belanger, S. Kraml and A. Pukhov, *Comparison of SUSY spectrum calculations and impact on the relic density constraints from WMAP*, *Phys. Rev.* **D 72** (2005) 015003 [hep-ph/0502079].

[12] T. Moroi, Y. Shimizu and A. Yotsuyanagi, *Reconstructing dark matter density with e^+e^- linear collider in focus-point supersymmetry*, *Phys. Lett.* **B 625** (2005) 79 [hep-ph/0505252].

[13] A. Birkedal et al., *Testing cosmology at the ILC*, hep-ph/0507214.

[14] M. Battaglia and M.E. Peskin, *The role of the ILC in the study of cosmic dark matter*, hep-ph/0509135.

[15] T. Moroi and Y. Shimizu, *Supersymmetric heavy Higgses at e^+e^- linear collider and dark-matter physics*, *Phys. Rev.* **D 72** (2005) 115012 [hep-ph/0509196].

[16] A. Birkedal, *Measuring dark matter at a collider*, *AIP Conf. Proc.* **805** (2006) 55 [hep-ph/0509199].

[17] M.M. Nojiri, G. Polesello and D.R. Tovey, *Constraining dark matter in the MSSM at the LHC*, *JHEP* **03** (2006) 063 [hep-ph/0512204].

[18] E.A. Baltz, M. Battaglia, M.E. Peskin and T. Wizansky, *Determination of dark matter properties at high-energy colliders*, *Phys. Rev.* **D 74** (2006) 103521 [hep-ph/0602187].

[19] M. Drees and C.-L. Shan, *Reconstructing the velocity distribution of WIMPs from direct dark matter detection data*, *JCAP* **06** (2007) 011 [astro-ph/0703651].

[20] A. Djouadi, *Dark matter and the ILC*, *Acta Phys. Polon.* **B37** (2006) 925 [hep-ph/0604107].

[21] M.J. White, *SUSY and dark matter constraints from the LHC*, hep-ph/0605065.

[22] S. Kraml, *LHC/ILC/cosmology interplay*, *Pramana* **67** (2006) 597 [hep-ph/0607270].

JHEP10(2007)016

[23] G. Servant and T.M.P. Tait, *Is the lightest Kaluza-Klein particle a viable dark matter candidate?*, *Nucl. Phys.* **B 650** (2003) 391 [hep-ph/0206071].

[24] H.-C. Cheng, J.L. Feng and K.T. Matchev, *Kaluza-Klein dark matter*, *Phys. Rev. Lett.* **89** (2002) 211301 [hep-ph/0207125].

[25] K. Agashe and G. Servant, *Warped unification, proton stability and dark matter*, *Phys. Rev. Lett.* **93** (2004) 231805 [hep-ph/0403143].

[26] K. Agashe and G. Servant, *Baryon number in warped GUTs: model building and (dark matter related) phenomenology*, *JCAP* **02** (2005) 002 [hep-ph/0411254].

[27] A. Birkedal-Hansen and J.G. Wacker, *Scalar dark matter from theory space*, *Phys. Rev.* **D 69** (2004) 065022 [hep-ph/0306161].

[28] H.-C. Cheng and I. Low, *TeV symmetry and the little hierarchy problem*, *JHEP* **09** (2003) 051 [hep-ph/0308199].

[29] E. Katz, J.-y. Lee, A.E. Nelson and D.G.E. Walker, *A composite little Higgs model*, *JHEP* **10** (2005) 088 [hep-ph/0312287].

[30] H.-C. Cheng and I. Low, *Little hierarchy, little Higgses and a little symmetry*, *JHEP* **08** (2004) 061 [hep-ph/0405243].

[31] A. Birkedal, A. Noble, M. Perelstein and A. Spray, *Little Higgs dark matter*, *Phys. Rev.* **D 74** (2006) 035002 [hep-ph/0603077].

[32] D. Stojkovic, G.D. Starkman and R. Matsuo, *Dark energy, the colored anti-de Sitter vacuum and LHC phenomenology*, hep-ph/0703246.

[33] R.R. Caldwell, R. Dave and P.J. Steinhardt, *Cosmological imprint of an energy component with general equation-of-state*, *Phys. Rev. Lett.* **80** (1998) 1582 [astro-ph/9708069].

[34] C. Wetterich, *Cosmologies with variable Newton's 'constant'*, *Nucl. Phys.* **B 302** (1988) 645.

[35] P.J.E. Peebles and B. Ratra, *Cosmology with a time variable cosmological 'constant'*, *Astrophys. J.* **325** (1988) 17.

[36] K. Freese, F.C. Adams, J.A. Frieman and E. Mottola, *Cosmology with decaying vacuum energy*, *Nucl. Phys.* **B 287** (1987) 797.

[37] O. Bertolami, *Time dependent cosmological term*, *Nuovo Cim.* **93** (1986) 36.

[38] W. Nahm, *Supersymmetries and their representations*, *Nucl. Phys.* **B 135** (1978) 149.

[39] P. Salati, *Quintessence and the relic density of neutralinos*, *Phys. Lett.* **B 571** (2003) 121 [astro-ph/0207396].

[40] M. Kamionkowski and M.S. Turner, *Thermal relics: do we know their abundances?*, *Phys. Rev.* **D 42** (1990) 3310.

[41] J.D. Barrow, *Massive particles as a probe of the early universe*, *Nucl. Phys.* **B 208** (1982) 501.

[42] D. Comelli, M. Pietroni and A. Riotto, *Dark energy and dark matter*, *Phys. Lett.* **B 571** (2003) 115 [hep-ph/0302080].

[43] F. Rosati, *Quintessential enhancement of dark matter abundance*, *Phys. Lett.* **B 570** (2003) 5 [hep-ph/0302159].

JHEP10(2007)016

[44] S. Profumo and P. Ullio, *SUSY dark matter and quintessence*, *JCAP* **11** (2003) 006 [hep-ph/0309220].

[45] R. Catena, N. Fornengo, A. Masiero, M. Pietroni and F. Rosati, *Dark matter relic abundance and scalar-tensor dark energy*, *Phys. Rev.* **D 70** (2004) 063519 [astro-ph/0403614].

[46] A. Masiero and F. Rosati, *Possible influence of dark energy on the dark matter relic abundance*, astro-ph/0501571.

[47] C. Pallis, *Quintessential kination and cold dark matter abundance*, *JCAP* **10** (2005) 015 [hep-ph/0503080].

[48] C. Pallis, *Kination dominated reheating and cold dark matter abundance*, *Nucl. Phys.* **B 751** (2006) 129 [hep-ph/0510234].

[49] M. Brhlik, D.J.H. Chung and G.L. Kane, *Weighing the universe with accelerators and detectors*, *Int. J. Mod. Phys.* **D 10** (2001) 367 [hep-ph/0005158].

[50] G. Barenboim and J.D. Lykken, *Minimal noncanonical cosmologies*, *JHEP* **07** (2006) 016 [astro-ph/0604528].

[51] G. Barenboim and J.D. Lykken, *Colliders as a simultaneous probe of supersymmetric dark matter and terascale cosmology*, *JHEP* **12** (2006) 005 [hep-ph/0608265].

[52] M. Drees, H. Iminniyaz and M. Kakizaki, *Constraints on the very early universe from WIMP dark matter*, arXiv:0704.1590.

[53] A. Birkedal, K. Matchev and M. Perelstein, *Dark matter at colliders: a model-independent approach*, *Phys. Rev.* **D 70** (2004) 077701 [hep-ph/0403004].

[54] J.L. Feng, A. Rajaraman and F. Takayama, *Superweakly-interacting massive particles*, *Phys. Rev. Lett.* **91** (2003) 011302 [hep-ph/0302215].

[55] J.L. Feng, A. Rajaraman and F. Takayama, *SuperWIMP dark matter signals from the early universe*, *Phys. Rev.* **D 68** (2003) 063504 [hep-ph/0306024].

[56] D.J.H. Chung, L.L. Everett and K.T. Matchev, *Inflationary cosmology connecting dark energy and dark matter*, arXiv:0704.3285.

[57] A.B. Lahanas, N.E. Mavromatos and D.V. Nanopoulos, *Smoothly evolving supercritical-string dark energy relaxes supersymmetric-dark-matter constraints*, *Phys. Lett.* **B 649** (2007) 83 [hep-ph/0612152].

[58] D.J.H. Chung, E.W. Kolb and A. Riotto, *Superheavy dark matter*, *Phys. Rev.* **D 59** (1999) 023501 [hep-ph/9802238].

[59] D.J.H. Chung, E.W. Kolb, A. Riotto and L. Senatore, *Isocurvature constraints on gravitationally produced superheavy dark matter*, *Phys. Rev.* **D 72** (2005) 023511 [astro-ph/0411468].

[60] E.W. Kolb and M.S. Turner, *The early universe*, Addison-Wesley, U.S.A. (1990).

[61] R.H. Cyburt, B.D. Fields, K.A. Olive and E. Skillman, *New BBN limits on physics beyond the standard model from He-4*, *Astropart. Phys.* **23** (2005) 313 [astro-ph/0408033].

[62] M. Battaglia et al., *Proposed post-LEP benchmarks for supersymmetry*, *Eur. Phys. J.* **C 22** (2001) 535 [hep-ph/0106204].

JHEP10(2007)016

[63] B.C. Allanach et al., *The snowmass points and slopes: benchmarks for SUSY searches*, in *Proc. of the APS/DPF/DPB Summer Study on the Future of Particle Physics*, Snowmass, Colorado, U.S.A., 30 Jun–21 Jul (2001), hep-ph/0202233

[64] M. Battaglia et al., *Updated post-WMAP benchmarks for supersymmetry*, *Eur. Phys. J.* **C 33** (2004) 273 [hep-ph/0306219].

[65] G. Belanger, F. Boudjema, A. Pukhov and A. Semenov, *micrOMEGAs: a program for calculating the relic density in the MSSM*, *Comput. Phys. Commun.* **149** (2002) 103 [hep-ph/0112278].

[66] G. Belanger, F. Boudjema, A. Pukhov and A. Semenov, *micrOMEGAs: version* 1.3, *Comput. Phys. Commun.* **174** (2006) 577 [hep-ph/0405253].

[67] G. Belanger, F. Boudjema, A. Pukhov and A. Semenov, *micrOMEGAs*2.0*: a program to calculate the relic density of dark matter in a generic model*, *Comput. Phys. Commun.* **176** (2007) 367 [hep-ph/0607059].

[68] F.E. Paige, S.D. Protopopescu, H. Baer and X. Tata, *ISAJET* 7.69*: a Monte Carlo event generator for pp, $\bar{p}p$ and e^+e^- reactions*, hep-ph/0312045.

[69] Y.M. Andreev, S.I. Bityukov and N.V. Krasnikov, *Sleptons at post-WMAP benchmark points at LHC(CMS)*, *Phys. Atom. Nucl.* **68** (2005) 340 [hep-ph/0402229].

[70] A. Birkedal, R.C. Group and K. Matchev, *Slepton mass measurements at the LHC*, in *Proceedings of 2005 International Linear Collider Workshop (LCWS 2005)*, Stanford, California, U.S.A. 18–22 Mar (2005), hep-ph/0507002.

[71] H. Baer, A. Belyaev, T. Krupovnickas and A. Mustafayev, *SUSY normal scalar mass hierarchy reconciles $(g-2)(\mu)$, $B \to S\gamma$ and relic density*, *JHEP* **06** (2004) 044 [hep-ph/0403214].

[72] J.L. Feng, K.T. Matchev and T. Moroi, *Multi-TeV scalars are natural in minimal supergravity*, *Phys. Rev. Lett.* **84** (2000) 2322 [hep-ph/9908309].

[73] J.L. Feng, K.T. Matchev and T. Moroi, *Focus points and naturalness in supersymmetry*, *Phys. Rev.* **D 61** (2000) 075005 [hep-ph/9909334].

[74] J.L. Feng and K.T. Matchev, *Focus point supersymmetry: proton decay, flavor and CP-violation and the Higgs boson mass*, *Phys. Rev.* **D 63** (2001) 095003 [hep-ph/0011356].

[75] J.L. Feng and F. Wilczek, *Advantages and distinguishing features of focus point supersymmetry*, *Phys. Lett.* **B 631** (2005) 170 [hep-ph/0507032].

[76] M.S. Carena and A. Freitas, *Collider searches and cosmology in the MSSM with heavy scalars*, *Phys. Rev.* **D 74** (2006) 095004 [hep-ph/0608255].

[77] J.L. Feng, K.T. Matchev and F. Wilczek, *Neutralino dark matter in focus point supersymmetry*, *Phys. Lett.* **B 482** (2000) 388 [hep-ph/0004043].

[78] U. Chattopadhyay, D. Choudhury, M. Drees, P. Konar and D.P. Roy, *Looking for a heavy Higgsino LSP in collider and dark matter experiments*, *Phys. Lett.* **B 632** (2006) 114 [hep-ph/0508098].

[79] P.G. Mercadante, J.K. Mizukoshi and X. Tata, *Using B-tagging to enhance the SUSY reach of the Cern large hadron collider*, *Phys. Rev.* **D 72** (2005) 035009 [hep-ph/0506142].

JHEP10(2007)016

[80] H. Baer, V. Barger, G. Shaughnessy, H. Summy and L.-t. Wang, *Precision gluino mass at the LHC in SUSY models with decoupled scalars*, *Phys. Rev.* **D 75** (2007) 095010 [hep-ph/0703289].

[81] R. Gray et al., *Measuring mass and cross section parameters at a focus point region*, hep-ex/0507008.

[82] H. Baer, T. Krupovnickas, S. Profumo and P. Ullio, *Model independent approach to focus point supersymmetry: from dark matter to collider searches*, *JHEP* **10** (2005) 020 [hep-ph/0507282].

[83] J.R. Ellis, T. Falk and K.A. Olive, *Neutralino stau coannihilation and the cosmological upper limit on the mass of the lightest supersymmetric particle*, *Phys. Lett.* **B 444** (1998) 367 [hep-ph/9810360].

[84] R. Arnowitt, B. Dutta, T. Kamon, N. Kolev and D. Toback, *Detection of SUSY in the stau-neutralino coannihilation region at the LHC*, *Phys. Lett.* **B 639** (2006) 46 [hep-ph/0603128].

[85] R. Arnowitt et al., *Measuring the stau - neutralino*(1) *mass difference in co-annihilation scenarios at the LHC*, hep-ph/0608193.

[86] P. Bambade, M. Berggren, F. Richard and Z. Zhang, *Experimental implications for a linear collider of the SUSY dark matter scenario*, hep-ph/0406010.

[87] V. Khotilovich, R. Arnowitt, B. Dutta and T. Kamon, *The stau neutralino co-annihilation region at an international linear collider*, *Phys. Lett.* **B 618** (2005) 182 [hep-ph/0503165].

[88] H. Baer et al., *Yukawa unified supersymmetric* SO(10) *model: cosmology, rare decays and collider searches*, *Phys. Rev.* **D 63** (2001) 015007 [hep-ph/0005027].

[89] J.R. Ellis, T. Falk, G. Ganis, K.A. Olive and M. Srednicki, *The CMSSM parameter space at large* $\tan\beta$, *Phys. Lett.* **B 510** (2001) 236 [hep-ph/0102098].

JHEP10(2007)016